SAND78-0815
Unlimited Release

Summary Report: Concentrating Solar Collector Test Results Collector Module Test Facility

Vernon E. Dudley, EG&G
Robert M. Workhoven

Prepared by Sandia Laboratories, Albuquerque, New Mexico 87185 and Livermore, California 94550 for the United States Department of Energy under Contract AT (29-1)-789
Printed May 1978

Sandia Laboratories

0 QD (4-78)

Printed in the United States of America

Available from
National Technical Information Service
U. S. Department of Commerce
5285 Port Royal Road
Springfield, VA 22161
Price: Printed Copy $5.25 ; Microfiche $3.00

Issued by Sandia Laboratories, operated for the United States
Department of Energy by Sandia Corporation

SAND 78-0815

Unlimited Release
Printed May 1978

SUMMARY REPORT:
CONCENTRATING SOLAR COLLECTOR TEST RESULTS, COLLECTOR MODULE TEST FACILITY

Vernon E. Dudley
EG&G, Inc.

Robert M. Workhoven
Midtemperature Solar Systems Facility Division 5712
Sandia Laboratories
Albuquerque, NM 87185

ABSTRACT

This report summarizes the results of tests on a series of five concentrating solar collectors from Suntec Systems, Inc,; Hexcel Corporation; General Atomic Company; McDonnell Douglas Astronautics Company; and Solar Kinetics, Inc. The Hexcel design performed better than the others primarily because of a highly reflective, precisely shaped mirror that focused almost all the reflected light onto the absorber. McDonnell Douglas, Suntec Systems, and Solar Kinetics designs were down about 10% in efficiency at temperatures near 300°C. The General Atomic FMSC performed at a lower level at low temperatures because of large reflected light spillover, but only about 3 to 4% lower than the others near operating temperatures of 300°C. Even the best of these collectors can be significantly improved.

CONTENTS

		Page
1.	INTRODUCTION	7
2.	TEST OBJECTIVE	7
3.	COLLECTOR DESCRIPTIONS	7
	3.1 SLATS, Suntec Systems, Inc.	8
	3.2 Parabolic Trough Concentrator, Hexcel Corporation	10
	3.3 FMSC, General Atomic Company	12
	3.4 Fresnel Lens Rotating Array Solar Collector, McDonnell Douglas	14
	3.5 Linear Parabolic Trough Concentrator, Solar Kinetics, Inc.	16
4.	PERFORMANCE TEST DEFINITIONS	19
5.	TEST RESULTS	21
	5.1 SLATS, Suntec Systems, Inc.	21
	5.2 Parabolic Trough Concentrator, Hexcel Corporation	21
	5.3 FMSC, General Atomic Company	29
	5.4 Fresnel Lens Rotating Array Solar Collector, McDonnell Douglas	29
	5.5 Linear Parabolic Trough Concentrator, Solar Kinetics, Inc.	38
6.	CONCLUSIONS	45
	REFERENCES	50

ILLUSTRATIONS

Figure		Page
1	SLATS Solar Collector	8
2	End View of SLATS Solar Collector	9
3	SLATS Reflector Assembly Cross Section	9
4	SLATS Receiver Assembly Cross Section	10
5	Hexcel Solar Collector	11
6	Cross Section of Hexcel Receiver Assembly	12
7	General Atomic FMSC	13
8	Annual and Daily Movement of FMSC Receiver	13
9	FMSC Heat Receiver Assembly Cross Section	14
10	McDonnell Douglas Linear Fresnel Lens Rotating Array Solar Collector	15
11	McDonnell Douglas Solar Collector	15
12	McDonnell Douglas Receiver Assembly	16
13	Solar Kinetics Solar Collector	17
14	Solar Kinetics Receiver Turbulence Generators	18
15	Typical Data Printout for Efficiency Test	20
16	Typical Data Printout for Thermal Loss Test	20
17	SLATS Efficiency vs. Output Temperature	22
18	SLATS Solar Noon Efficiency	23
19	SLATS Receiver Thermal Loss	24
20	Thermal Conductivity Comparison of Different Insulation Materials	25
21	Hexcel Collector Efficiency vs. Output Temperature	26
22	Hexcel Solar Noon Efficiency	27
23	Hexcel All Day Efficiency	28
24	Hexcel Receiver Thermal Loss	30
25	GA FMSC Efficiency vs. Output Temperature	31
26	GA FMSC Solar Noon Efficiency	32
27	Light Intensity Scans Across FMSC Receiver Aperture	33
28	GA FMSC Receiver Thermal Loss	34
29	McDonnell Douglas Efficiency vs. Output Temperature	35
30	McDonnell Douglas Collector Solar Noon Efficiency	36
31	McDonnell Douglas All Day Efficiency at 250°C	37
32	McDonnell Douglas Receiver Thermal Loss	39
33	Solar Kinetics Efficiency vs. Output Temperature	40
34	Solar Kinetics Collector Solar Noon Efficiency	41
35	Solar Kinetics All Day Efficiency	42
36	Solar Kinetics Receiver Thermal Loss	44
37	Comparison of Solar Noon Efficiency vs. Output Temperature	46
38	Comparison of Solar Noon Efficiency	47
39	Comparison of Thermal Loss Per Meter of Receiver Length	48
40	Comparison of Thermal Loss Per Unit Area Collector Aperture	49

SUMMARY REPORT:
CONCENTRATING SOLAR COLLECTOR TEST RESULTS,
COLLECTOR MODULE TEST FACILITY

1. INTRODUCTION

A series of concentrating solar collectors have been tested at Sandia Laboratories' Collector Module Test Facility (CMTF). This facility is part of the Mid-temperature Solar Systems Test Facility (MTSSTF), and is operated under the Department of Energy's continuing program to characterize selected collector modules for possible future systems use (see Reference 1). The solar collectors tested may have important commercial applications in replacing fossil-fuel energy sources with solar thermal power systems for irrigation pumping, electric-utility power generation, combined electric power and heat energy (total energy systems), and as a source for high-temperature process heat.

Five collector modules were tested between August 1977 and January 1978. The sponsoring companies and their collectors are: 1) Suntec Systems, Inc., Solar Linear Array Thermal System (SLATS); 2) Hexcel Corp., a parabolic trough concentrator; 3) General Atomic Co., Fixed Mirror Solar Concentrator (FMSC); 4) McDonnell Douglas Astronautics Co., Fresnel lens rotating array solar collector, and 5) Solar Kinetics, Inc., Model T-500, a linear parabolic trough concentrator. The Suntec SLATS used pressurized water as a heat transfer fluid; the others used Therminol 66.

2. TEST OBJECTIVE

The objective of this test series was to characterize the performance of concentrating solar collectors. Of primary concern were the thermal efficiency and thermal losses of these collectors over a temperature range from about 150°C to 300°C.

3. COLLECTOR DESCRIPTIONS

Table I summarizes the collector characteristics of the five modules tested at Sandia. Detailed descriptions for each collector are given in this section.

Table 1. Collector Characteristics.

Collector	Aperture Area (m^2)	Secondary Aperture (cm)	Receiver Length (m)	Focal Length (cm)	Concentration Ratio	Reflector Surface
Suntec	35.97	8.64	12.20	305.0	35:1	Glass
General Atomic	16.26	5.10	7.16	302.0	43:1	Glass
Hexcel	15.91	--	6.40	91.4	67:1	FEK-163 acrylic
McDonnell Douglas	15.54	7.80	17.34	92.7	24:1	Cast acrylic Fresnel lens*
Solar Kinetics	12.7	--	12.20	26.7	41:1	FEK-244 acrylic

*Transmission lens

3.1 SLATS, SUNTEC SYSTEMS, INC.

The Suntec SLATS system is a linear Fresnel reflector system consisting of two bays of 10 reflectors each, a supporting structure, and a fixed receiver assembly. Figure 1 shows the collector system installed at Sandia. Figure 2 is an end view of the collector module showing the orientation of the individual reflectors and the receiver assembly. Note that each individual reflector is set at a slightly different angle so that reflected sunlight from all the reflectors converges on the fixed receiver aperture. The individual reflectors are mechanically linked together and are rotated on command of the sun tracking system to focus on the receiver. When not in operation, the reflectors are rotated to a face-down position. Figure 3 shows the reflector cross section.

The receiver assembly (see Figure 4 for cross section) is a double pass system, with the heat-transfer fluid entering one end of the receiver, passing the length of the receiver through one absorber tube, then traveling through a turnaround at the end and back across the receiver through the second absorber tube. The absorber tubes were plated with a selective black chrome to enhance solar absorption and minimize radiation thermal losses.

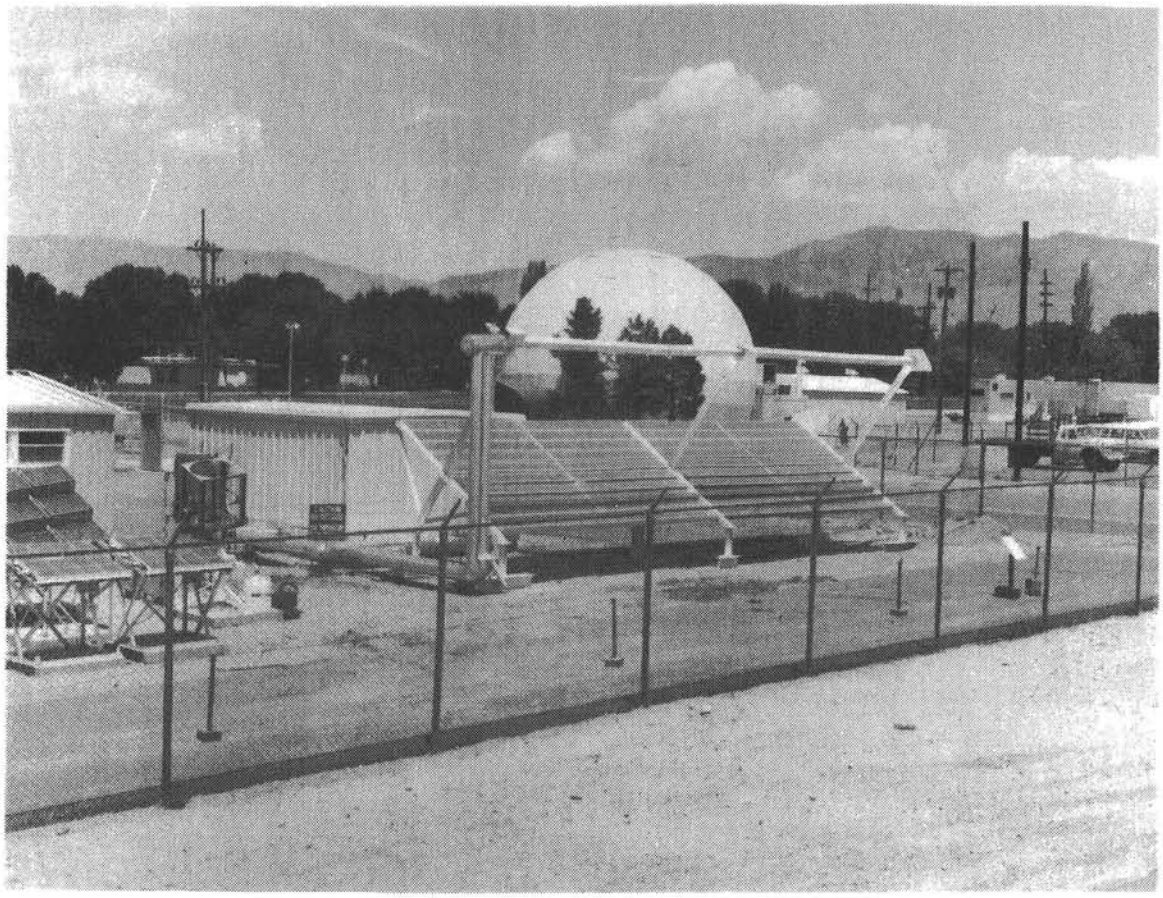

Figure 1. SLATS Solar Collector.

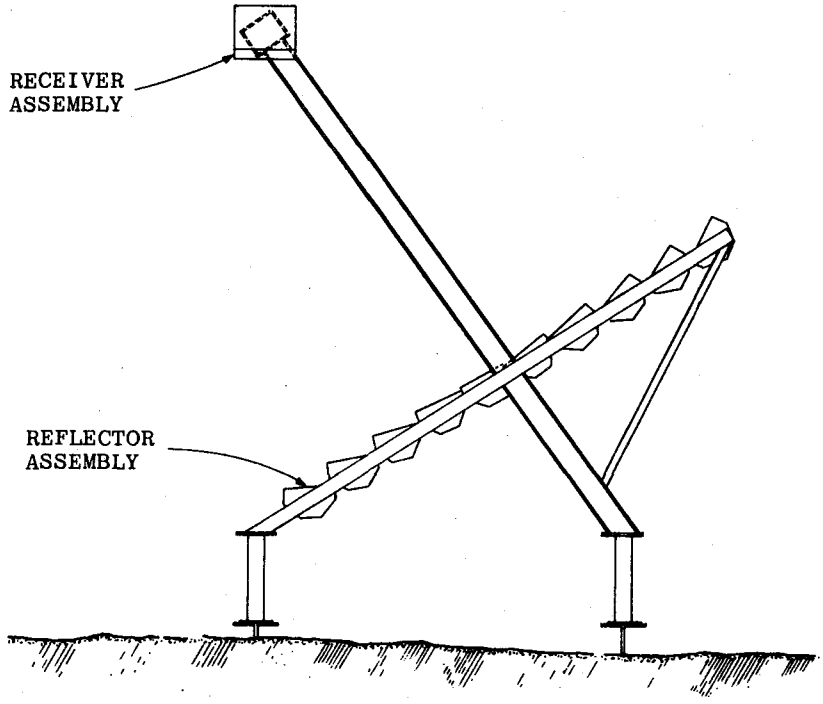

Figure 2. End View of SLATS Solar Collector.

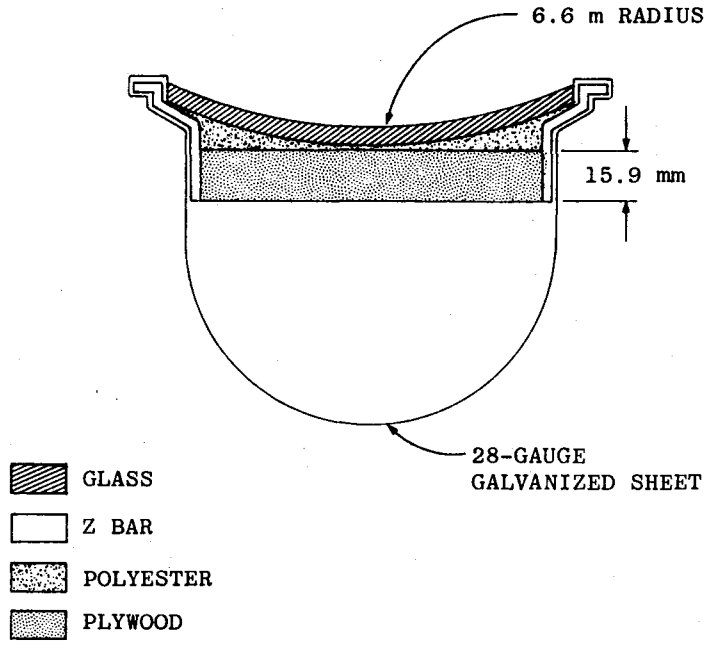

Figure 3. SLATS Reflector Assembly Cross Section.

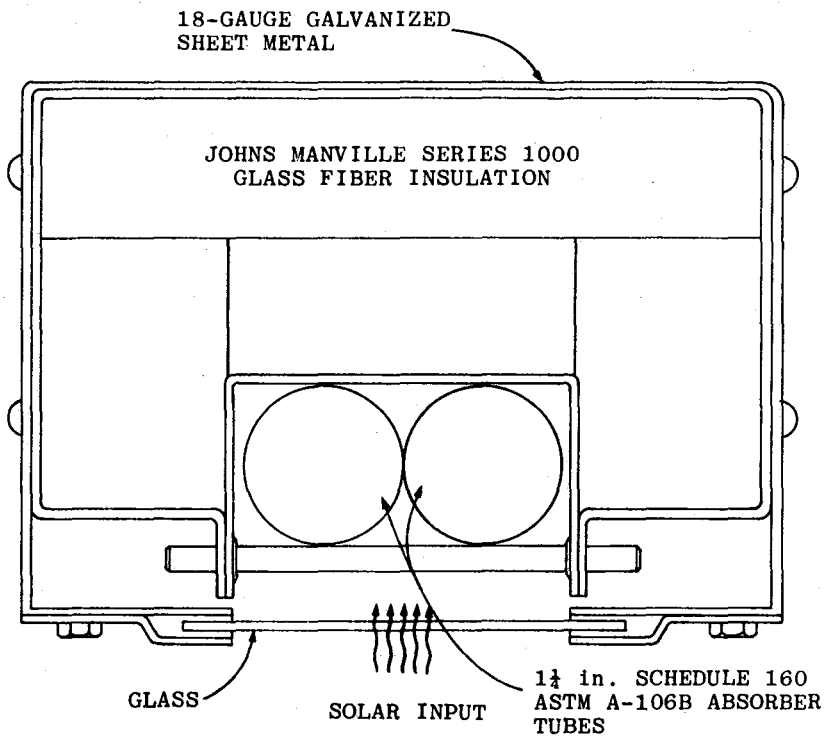

Figure 4. SLATS Receiver Assembly Cross Section.

The SLATS solar collector could be designed to use a low-pressure, synthetic-oil heat-transfer fluid; however, as tested at the CMTF it was configured for use with 330°C water pressurized at 18.3 MPa.

The SLATS collector was tested on CMTF's Fluid Loop 3, which supplies controlled-temperature pressurized water as a heat-transfer fluid at temperatures from about 120°C to 330°C. Design fluid flow rates range from 0.4 to 40 liters/min. Operating pressure is 18.3 MPa (2650 psig). Details concerning the design, construction, and operation of the CMTF fluid Test Loop 3 can be found in Reference 2.

Preliminary analysis of the SLATS test results through October 1977 has been published by Suntec Systems, Inc. (Reference 3). This summary report includes test results obtained through February 1978. A final report will be issued by Sandia when additional high-temperature (330°C) testing is completed, probably in the third quarter of 1978 (see Reference 4).

3.2 PARABOLIC TROUGH CONCENTRATOR, HEXCEL CORP.

The Hexcel solar concentrator used four aluminum honeycomb mirror panels arranged to form a linear focus parabolic reflector (see Figure 5). The reflecting surface was FEK 163 - an aluminized second-surface, acrylic film manufactured by the 3M Corp.

The black-chrome-plated absorber was a steel tube 3.81 cm in outside diameter. The absorber tube had internal fins and a 3.02 cm diameter internal plug tube to

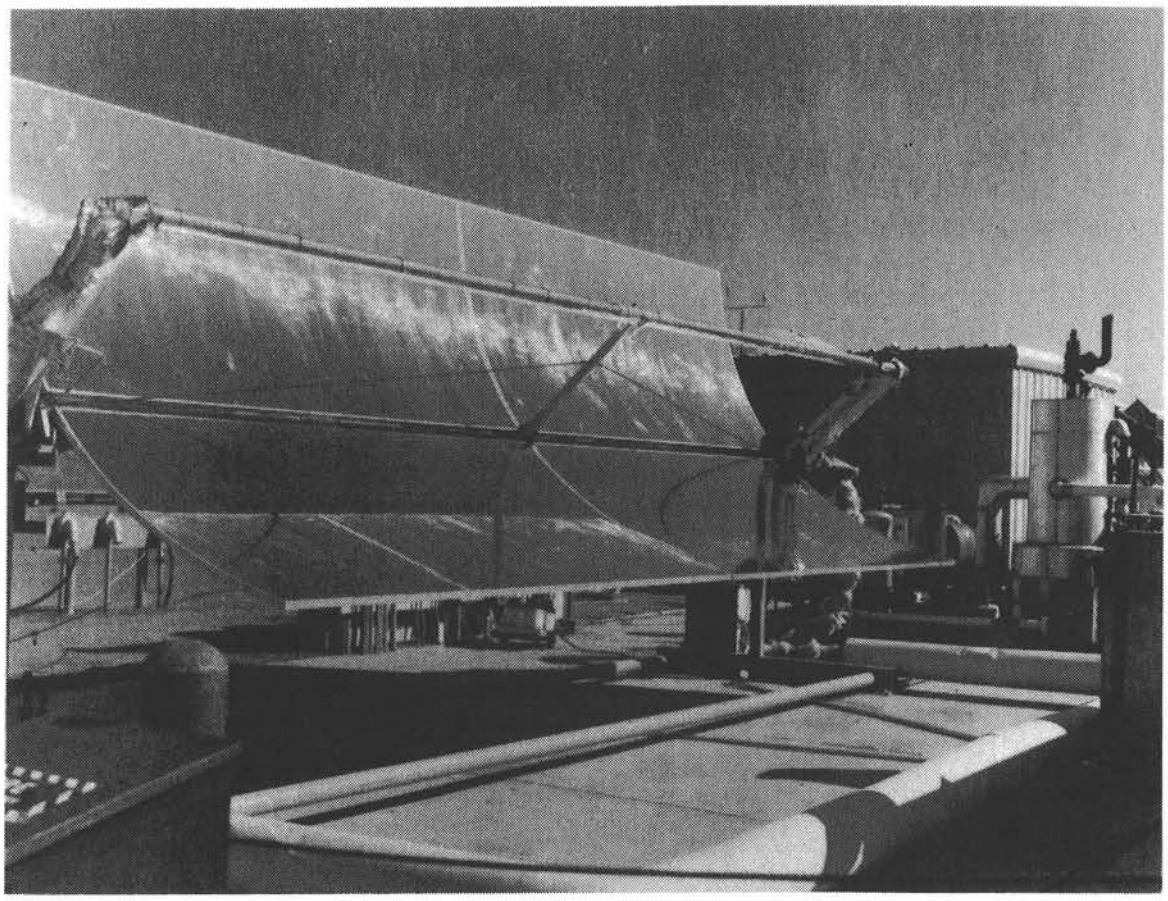

Figure 5. Hexcel Solar Collector.

confine the fluid flow to the tube wall area and improve heat-transfer characteristics. To reduce conduction and convection losses, a half-cylinder of Pyrex glass was fitted over the absorber tube on the radiation absorbing side. The back half of the tube was covered with a double-layer metal shield. The inner surface of the metal cover was polished aluminum to serve as a secondary concentrator; insulation was placed between the two layers. See Figure 6 for a cross section of the Hexcel receiver assembly.

The Hexcel collector and all the other collectors except the Suntec SLATS were tested on the CMTF's Fluid Loop 1. This fluid-loop system delivers Therminol 66, a synthetic heat-transfer oil, (see Reference 5) at a controlled temperature and flow rate. Inlet fluid temperatures range from about 75°C to 300°C at flow rates from 4 to 40 liters/min. Details of the construction and operation of the fluid loop system can be found in Reference 6.

The Hexcel Corporation has completed analysis of test results (see Reference 7). A Sandia Test Report has also been published (see Reference 8).

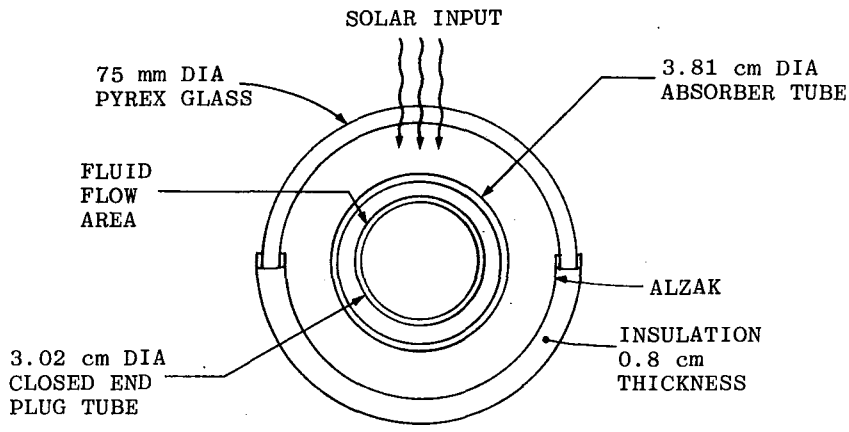

Figure 6. Cross Section of Hexcel Receiver Assembly.

3.3 FMSC, GENERAL ATOMIC COMPANY

The General Atomic Fixed Mirror Solar Concentrator (FMSC) is a concave array of long, narrow, flat mirror facets fixed on a segment of a cylindrical surface. Figure 7 is a photograph of the GA FMSC collector installed at the CMTF. The array of flat reflecting facets produces a narrow focal line that follows a circular path as the sun moves. Because the focal line path is on the same basic cylindrical surface as the mirror facets, the focal line can be tracked by a movable heat-receiver assembly that rotates about the center of curvature of the reflector module.

One mirror facet near the center of the module is tangent to the basic cylindrical curvature of the module. The remaining mirror facets are set at different angles such that all reflect incident light to the focal point. See References 9 and 10 for a more complete description of the optical principles of the FMSC.

The FMSC modules tested at the CMTF were constructed from reinforced cast concrete. The concrete modules were cast over a precision metal mold. A transferable film adhesive was used to fasten the 43 second-surface, silvered-glass mirror facets to the concrete surface.

The FMSC heat receiver assembly moved along a circular path to track the reflector focal point; Figure 8 illustrates the movement of the receiver around the reflector at different times of the day and year. In all positions, the receiver is aimed at the tangent mirror facet.

The internal construction of the FMSC receiver assembly is quite different from that of the Suntec SLATS receiver (see Figure 9 for a cross-sectional view). The black-chrome-plated absorber tube was a flattened oval supported inside by an aluminum channel enclosure and surrounded by a highly effective silica-foam insulation. The secondary concentrators had polished-aluminum mirrors on their inner surfaces to assist in concentrating sunlight onto the absorber surface.

General Atomic has completed preliminary analysis of the FMSC test results (Reference 9), and a Sandia report of test results has also been completed (Reference 11).

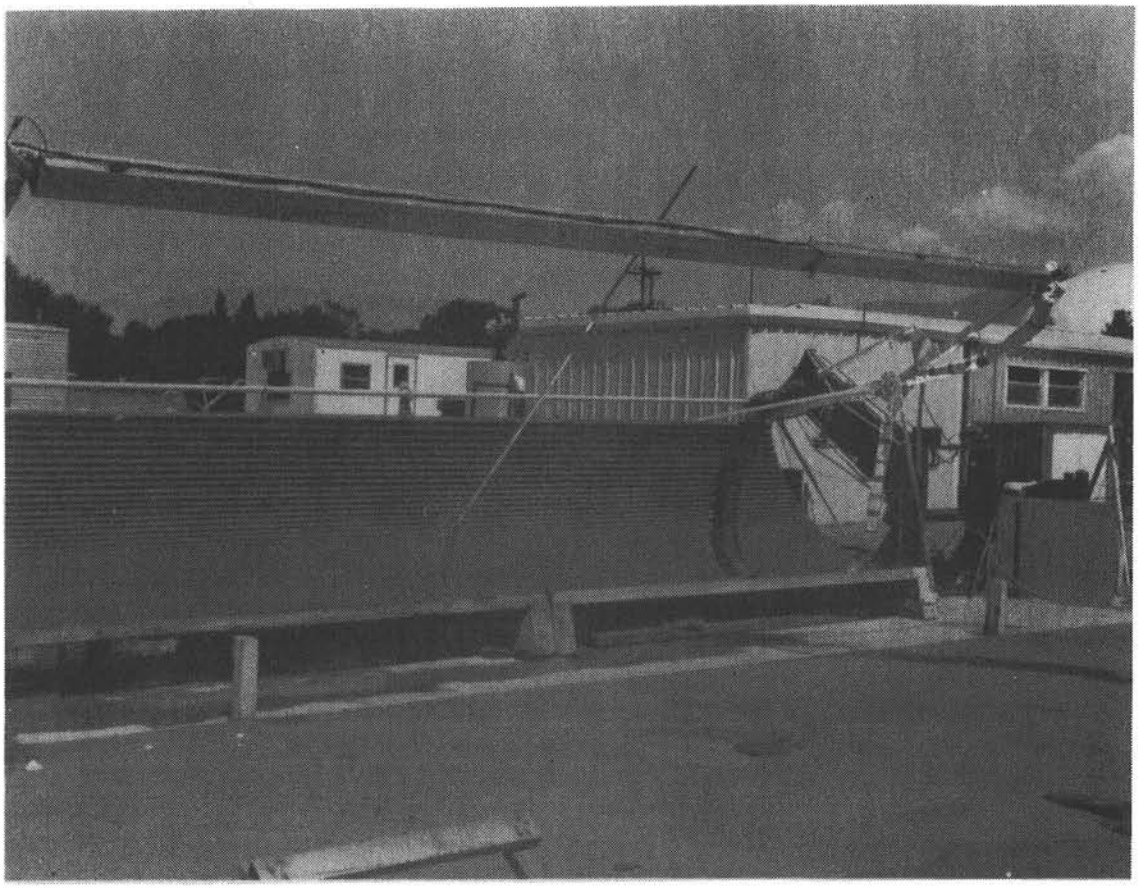

Figure 7. General Atomic FMSC.

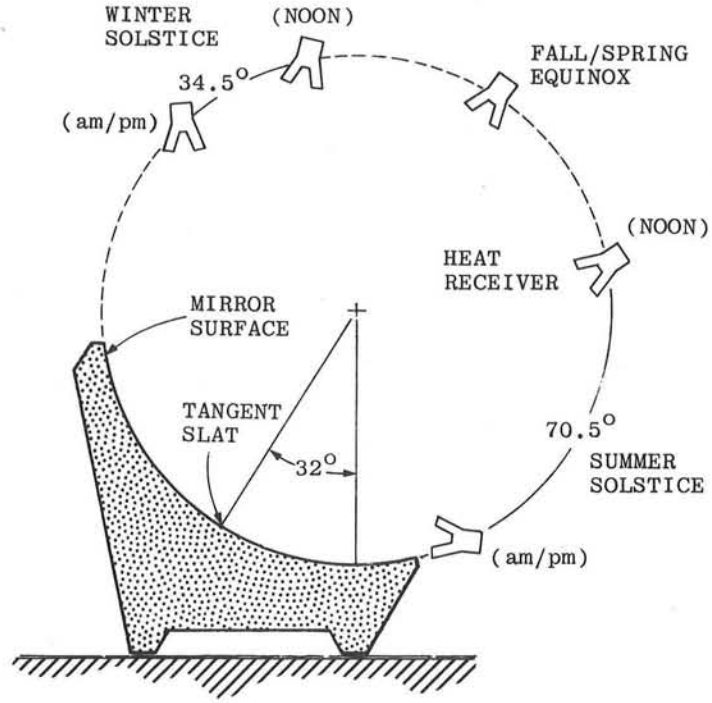

Figure 8. Annual and Daily Movement of FMSC Receiver.

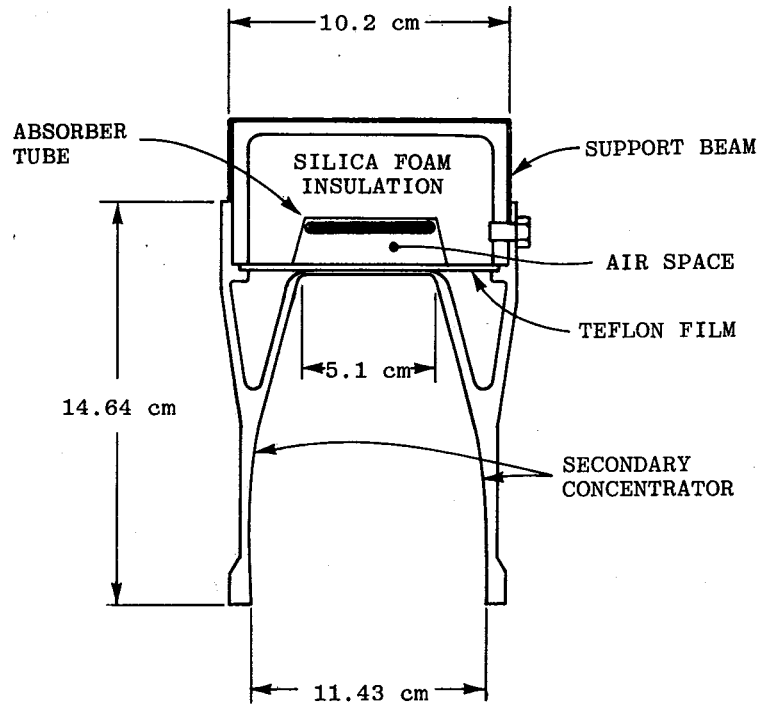

Figure 9. FMSC Heat Receiver Assembly Cross Section.

3.4 FRESNEL LENS ROTATING ARRAY SOLAR COLLECTOR, McDONNELL DOUGLAS CO.

The McDonnell Douglas Fresnel Lens Rotating Array Solar Collector used cast acrylic, linear Fresnel lenses to concentrate sunlight upon a series of absorber tubes. The collector was an aluminum box 5.94 m long x 3.63 m wide x 1.07 m deep. It was mounted on a pedestal to allow full sun tracking in both azimuth and elevation. Figure 10 is a photograph of the collector. The front illuminated face of the collector was a series of eight sections of linear Fresnel lenses focusing sunlight on four receiver assemblies within the box (see Figure 11). For fluid flow, the four individual absorber tubes contained an inner plug tube to confine the fluid flow to the wall area of the absorber.

The receiver assemblies, shown in cross section in Figure 12, contained a black-chrome-plated, steel absorber tube; secondary reflectors to aid in capturing stray sunlight; and a low-iron glass cover to minimize thermal convection losses. The whole receiver assembly was insulated with glass fiber batts and glass cloth.

Test results from the McDonnell Douglas Fresnel lens collector are being analyzed and a report is in preparation (see Reference 12).

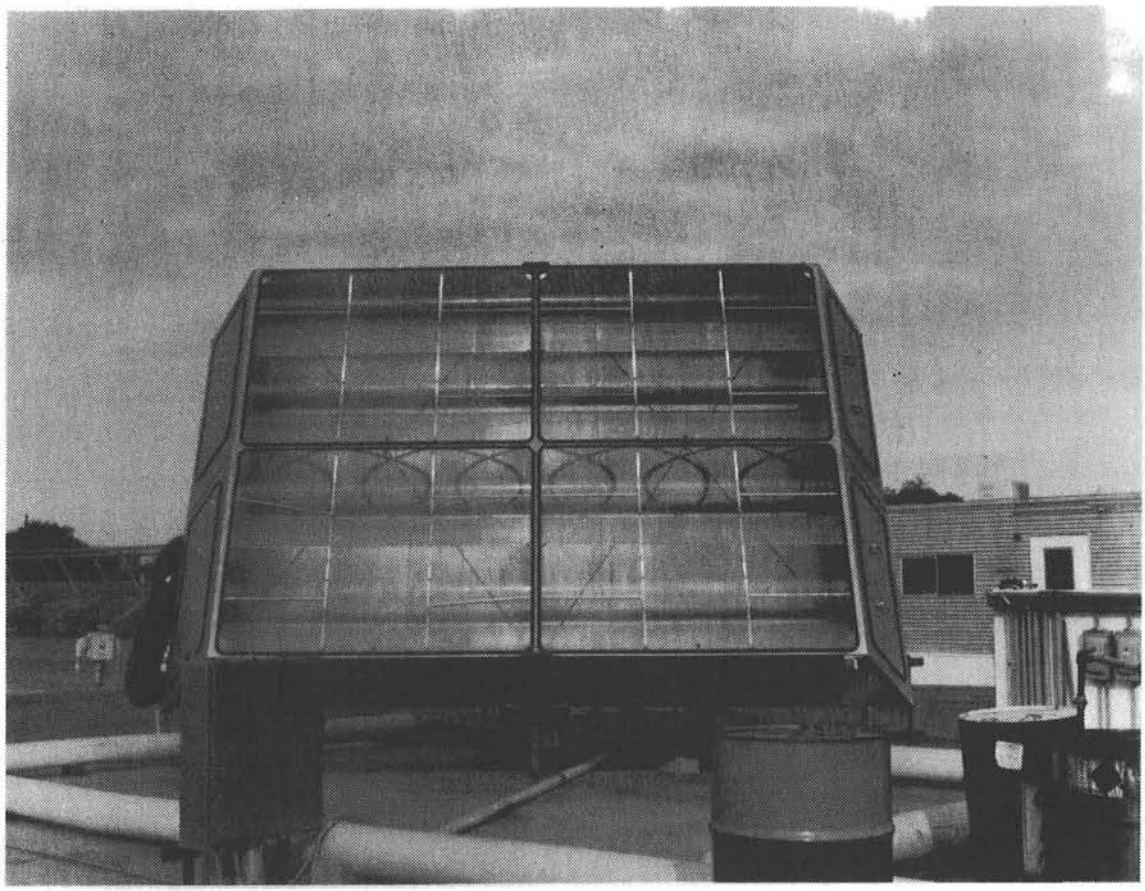

Figure 10. McDonnell Douglas Linear Fresnel Lens Rotating Array Solar Collector.

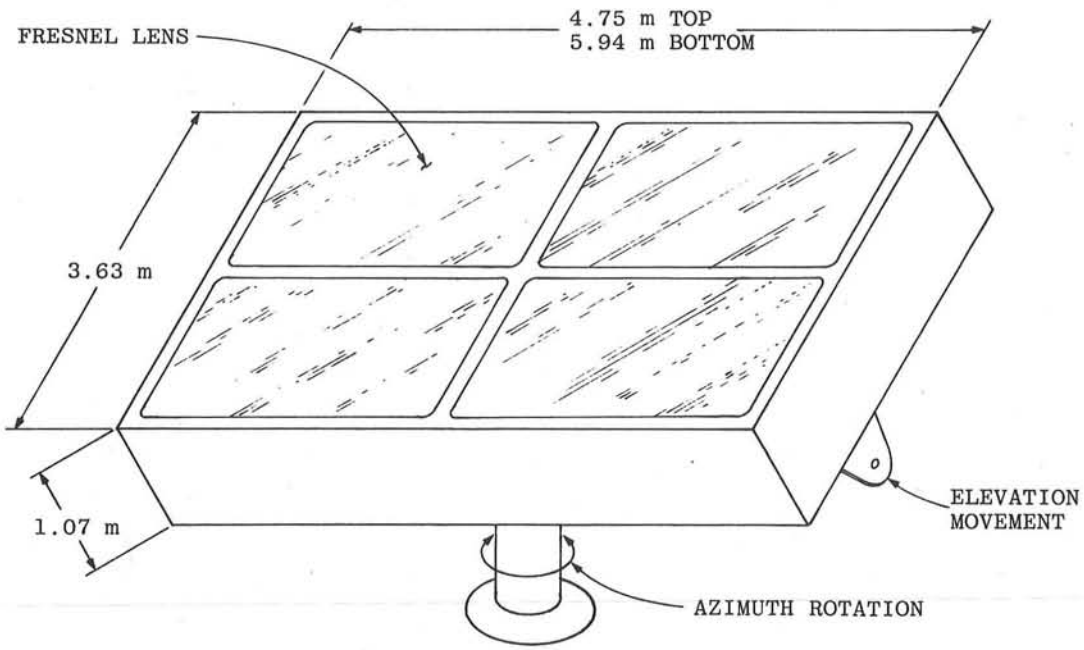

Figure 11. McDonnell Douglas Solar Collector.

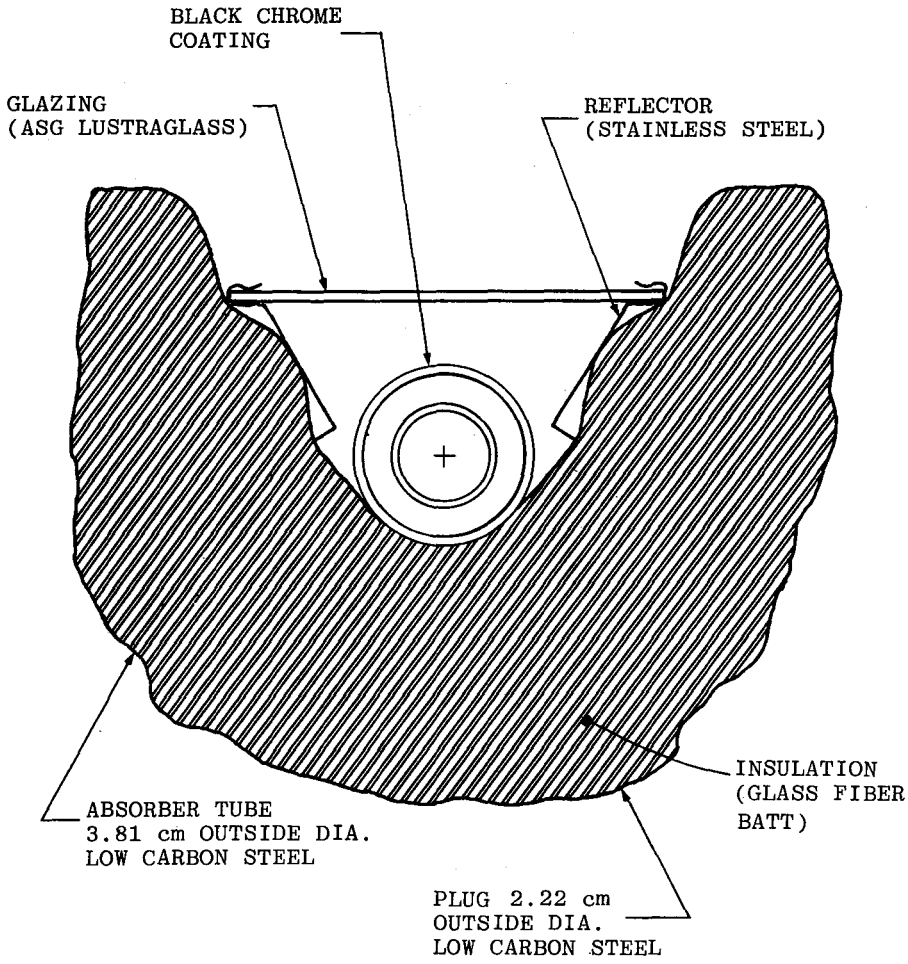

Figure 12. McDonnell Douglas Receiver Assembly.

3.5 LINEAR PARABOLIC TROUGH CONCENTRATOR, SOLAR KINETICS, INC.

The Solar Kinetics Model T-500 solar collector is a linear parabolic trough concentrator. The parabolic mirrors were constructed in 6.1 m lengths; two of these mirrors were placed end-to-end to form a row 12.2 m long for testing at Sandia. Two such rows were tested; the configurations of the two rows were not identical. A photograph of the Solar Kinetics installation at the CMTF is shown in Figure 13.

The linear parabolic mirror was an aluminum monocoque construction. Precision aluminum castings were used for internal bulkheads, and the skin was 18-gauge, heat-treated, T6 aluminum sheet. The reflective surface was FEK-244, a second-surface, aluminized-acrylic film by the 3M Co.

Figure 13. Solar Kinetics Solar Collector.

The Solar Kinetics receiver assembly consisted of a black-chrome-plated steel tube inside a Pyrex glass tube. The absorber tube was 2.54 cm in diameter. Four different internal configurations were tested (see Figure 14):

1) an empty tube,
2) the tube with a flat, twisted tape spiraling down the center of the tube,
3) a spiral spring along the inner tube wall,
4) both the spring and the twisted tape.

The purpose of these different absorber configurations was to determine any efficiency difference due to greater fluid flow turbulence and the effect these configurations would have on the pumping pressure required to achieve the desired flow rates.

Two variations in the Pyrex glass absorber tube cover were also tested. One collector row was fitted with a glass tube of 5.08 cm inside diameter and the other row with a glass tube of 4.45 cm inside diameter. Losses and efficiency were then measured for each receiver assembly with air, argon, or a vacuum in the annulus space between the absorber tube and the glass tube cover.

All the other collectors tested used electric motors for obtaining mechanical motion for sun tracking; Solar Kinetics used a hydraulic system. The hydraulic system had a unique advantage: sufficient hydraulic fluid was stored under pressure in an accumulator to drive the system out of focus in case of power failure that would cause a loss of fluid flow through the receiver.

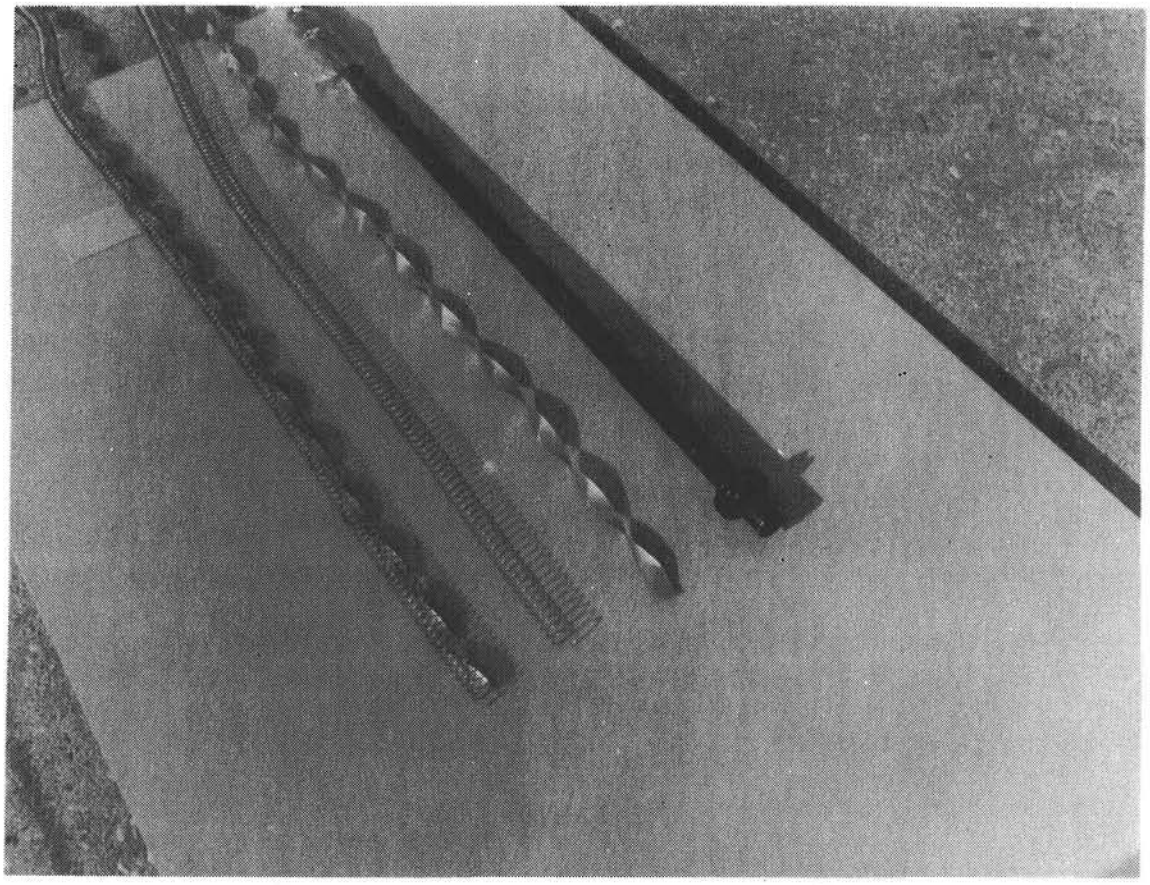

Figure 14. Solar Kinetics Receiver Turbulence Generators.

4. PERFORMANCE TEST DEFINITIONS

Two performance tests were of primary importance. These were the peak thermal efficiency at solar noon and the receiver thermal loss.

Heat gain (or loss) was calculated from

$$Q = \dot{m}\, C\, \Delta T$$

where

Q = heat gain, kJ/hr

$\dot{m}$ = mass flow rate of fluid, kg/hr

C_p = specific heat of fluid, kJ/kg, °C

ΔT = in/out temperature differential, °C

The flow rate and temperatures of the heat-transfer fluid were measured; density and specific heat were calculated from the average receiver temperature.

Efficiency was calculated from

$$\eta = \frac{Q/A}{I}$$

where

η = solar collector efficiency

Q = heat gain, W

A = collector aperture area, m^2

I = insolation, W/m^2

Loss measurements were normally made in the morning until about 1 hour before noon. For complete temperature and flow stabilization, efficiency testing was conducted at a single temperature and flow rate from about 1 hour before noon until about 1 hour after noon. This procedure ensured good definition of the peak noon efficiency. Loss testing was then resumed for the rest of the day. All-day efficiency tests were an exception to the above procedures; these were run continuously all day at a constant flow rate and constant input temperature to define the concentrator's efficiency with varying insolation and changing sun angles.

Figure 15 is a sample of the data obtained during an efficiency test; Figure 16 is a sample of thermal loss data. Blocks of data such as these were obtained about every 3 minutes during a test run. A "good" efficiency data point consists of at least one of these 10-point averaged data blocks, obtained near solar noon, during which input and output temperatures changed by 0.1°C or less, flow rate varied by 0.1 liter/min or less, delta temperature remained within 0.1°C or less, and insolation was above 950 W/m and constant to about 1%.

The magnitude of the solar radiation was not quite so important for loss testing, but losses do vary with insolation, therefore a reasonably high and steady solar input was required for a "good" loss data point. Other requirements for a loss test were the same as for efficiency testing.

In addition to the above, temperatures, flow rate, insolation, etc., had to be nearly as stable as described for at least 5 to 10 minutes before the "good" data point to be believable. In most cases, every effort was made to maintain stable conditions for about 30 minutes.

Efficiency and loss measurements were supplemented as required with measurements from other tests to define the collector's advantages and shortcomings. In most cases, measurements were made of the absorptance and emissivity of the absorber surface. When possible, differential pressure measurements were made over a range of flow rates to ascertain the pumping power requirements.

SOLAR KINETICS COLLECTOR EFFICIENCY TEST

JULIAN DAN 7 HOUR 12 MINUTE 54 (SOLAR TIME)

6.61 (DEG C) AMBIENT TEMPERATURE (DEG F) 43.9
133 WIND DIRECTION, DEGREES
10 WIND SPEED, MPH

******NORTH COLLECTOR ONLY******

TEMP IN	TEMP OUT	SOLAR WATTS/M^2	DELTA TEMP	FLOW LITERS/MIN	EFFICIENCY PERCENT
264.72	273.39	1037.1	8.76	19.14	42.6
264.72	273.33	1038.4	8.75	19.14	42.5
264.72	273.33	1039.2	8.66	19.13	42
264.72	273.33	1039.6	8.76	19.1	42.4
264.72	273.33	1041	8.52	19.15	41.3
264.72	273.33	1045.1'	8.69	19.15	41.9
264.72	273.39	1044.7	8.71	19.15	42.1
264.72	273.39	1044.6	8.78	19.11	42.3
264.72	273.33	1043.1	8.76	19.14	42.3
264.67	273.28	1041.3	8.71	19.15	42.2
		10 POINT AVERAGES			
264.715	273.343	1041.41	8.71	19.136	42.16

AVG EFFICIENCIES: N= 42.16 S= 47.81 TOTAL= 42.69

Figure 15. Typical Data Printout for Efficiency Test.

SOLAR KINETICS THERMAL LOSS TEST

JULIAN DAY 357 HOUR 14 MINUTE 18 (SOLAR TIME)

11.33 (DEG C) AMBIENT TEMPERATURE (DEG F) 52.4
24 WIND DIRECTION, DEGREES
10 WIND SPEED, MPH

*****SOUTH COLLECTOR LOSS ONLY*****

TEMP IN	TEMP OUT	FLOW LITERS/MIN	DELTA TEMP	WATTS GAIN/LOSS
175.56	174.5	19.06	-.89	-524.903
175.56	174.56	19.04	-.91	-536.154
175.56	174.56	19.03	-.93	-547.683
175.61	174.56	19.04	-.89	-524.403
175.56	174.56	19.04	-.91	-536.154
175.56	174.56	19.05	-.95	-559.989
175.56	174.5	19.02	-.97	-570.935
175.56	174.5	19.03	-.97	-571.185
175.56	174.56	19.04	-.99	-583.297
175.56	174.56	19.05	-.91	-536.404
	10 POINT AVERAGES			
175.565	174.542	19.04	-.932	-549.111

Figure 16. Typical Data Printout for Thermal Loss Test.

5. TEST RESULTS

5.1 SLATS, SUNTEC SYSTEMS, INC.

Figure 17 shows efficiency data accumulated to date as a function of output temperature. Figure 18 is the same efficiency data plotted as a function of average receiver fluid temperature above ambient temperature divided by direct insolation. Because of instabilities in temperature and flow-rate control systems, the data on the Suntec collector are not considered "good" data, as defined earlier. These instabilities probably caused some of the scatter in the data shown in Figure 17. The curve, however, is believed to be a reasonable representation of the collector's performance. Additional testing is planned after modifications to improve the fluid loop control systems. Additional testing will also extend high-temperature efficiency measurements to about 340°C.

Two data points in Figure 17 illustrate the effect of an accumulation of dust and dirt on the mirror surfaces of the collectors. A decrease in efficiency of about 6% is typical of effects seen on several other collectors.

Initial measurements on SLATS were made with an aluminized Teflon film on the reflector surfaces; these reflectors were unsatisfactory due to problems with mechanical precision and poor specular reflectivity. As a result of the preliminary tests, new reflectors were installed using silvered glass and a different mechanical design (see Figure 3). All data used in this report were obtained using the glass mirrors.

The glass mirror reflectors installed were not of the best quality, but were leftovers from construction of the 260 m^2 SLATS field installed at the Sandia Mid-temperature Solar Systems Test Facility. The focal pattern from these reflectors is not optimum; light spills over both sides of the receiver assembly. Attempts have been made to correct this spillover, and further corrections will be made to improve the SLATS efficiency.

Figure 19 shows the thermal loss measured in the SLATS receiver as a function of temperature. Loss is shown in watts(W), W/m length of receiver, and in W/m^2 of collector aperture. The curve is a least-squares fit to the data. These losses are relatively high. The receiver assembly (Figure 4) had a relatively wide aperture because of the two side-by-side absorber tubes; this tends to increase radiation losses. In addition, the glass-fiber batt insulation is not as effective as some other insulations (see Figure 20).

5.2 PARABOLIC TROUGH CONCENTRATOR, HEXCEL CORPORATION

Figure 21 shows the measured efficiency of the Hexcel linear parabolic trough solar collector. Figure 22 is the same efficiency data plotted as a function of average receiver fluid temperature above ambient temperature divided by direct insolation. The efficiency of this collector was the highest yet measured at the CMTF (this is probably due to the quality of the mirror surface and the accuracy of the focal line). Virtually no light missed the absorber tube. No dependance of efficiency on fluid flow rate could be detected. Figure 23 shows the Hexcel all day efficiency.

Measurements of the absorptance and emittance on Hexcel's black-chrome-plated absorber tube indicated that the absorptance was not optimum before testing began at the CMTF (Reference 8). The absorptance decreased further during the test series,

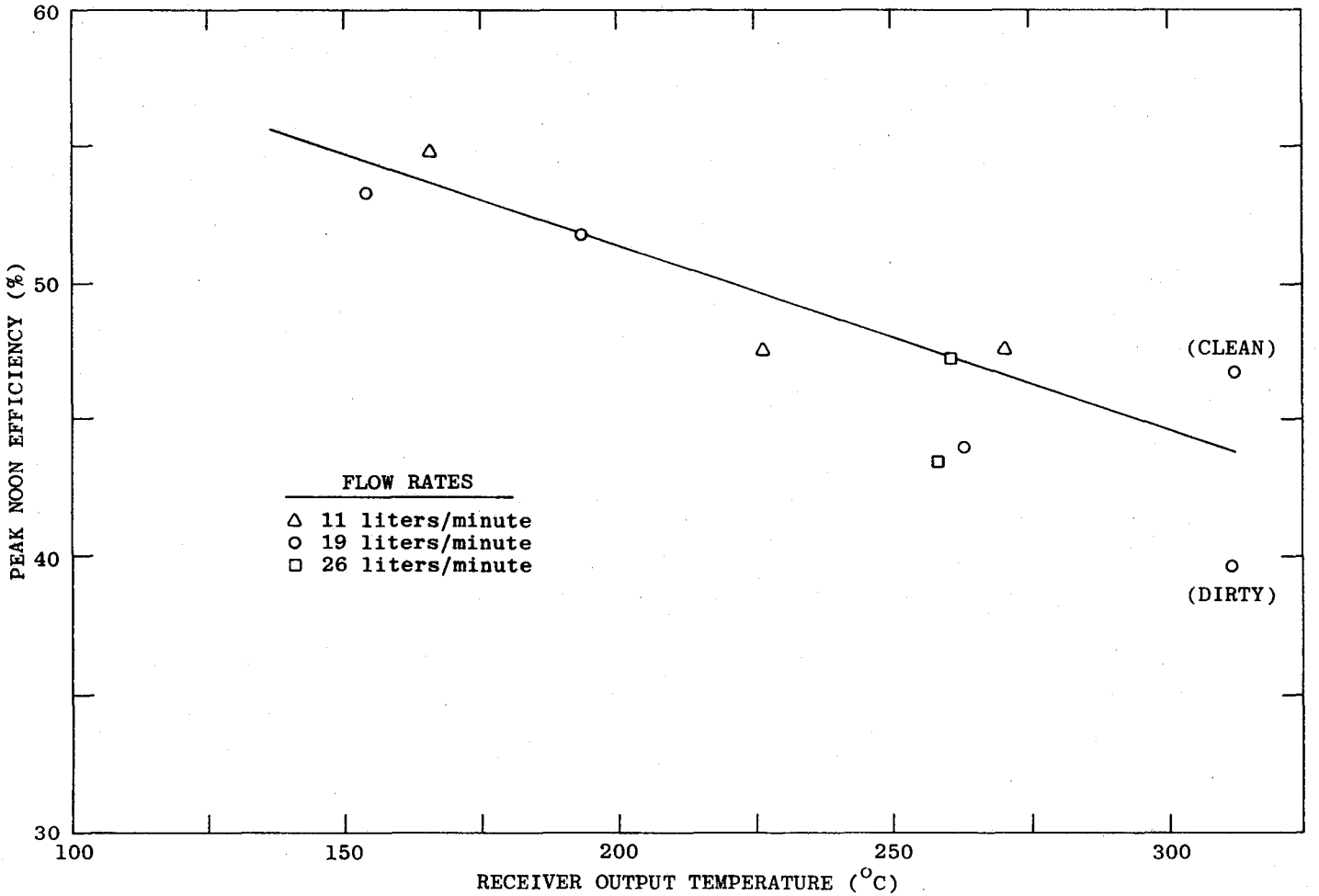

Figure 17. SLATS Efficiency vs. Output Temperature.

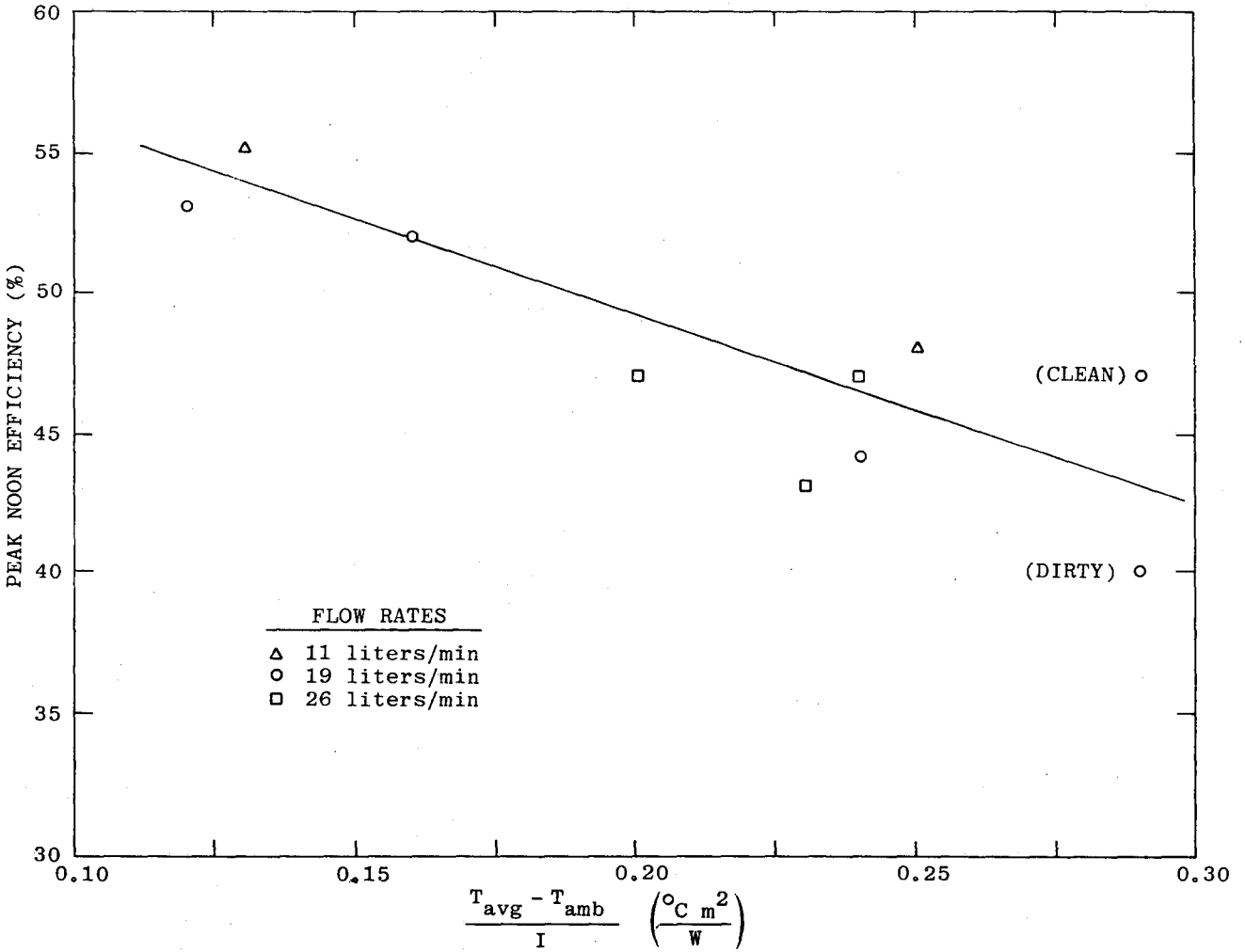

Figure 18. SLATS Solar Noon Efficiency.

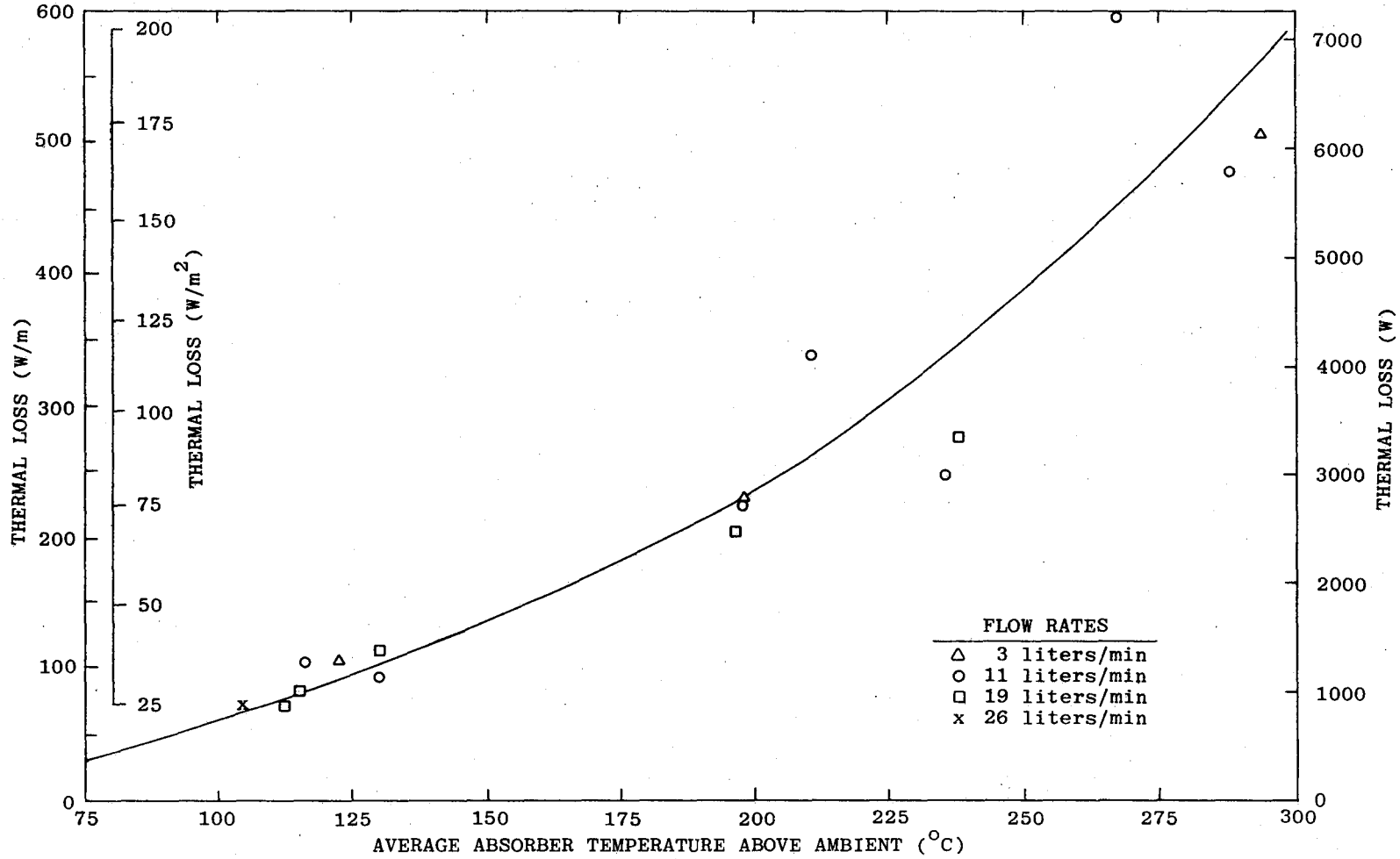

Figure 19. SLATS Receiver Thermal Loss.

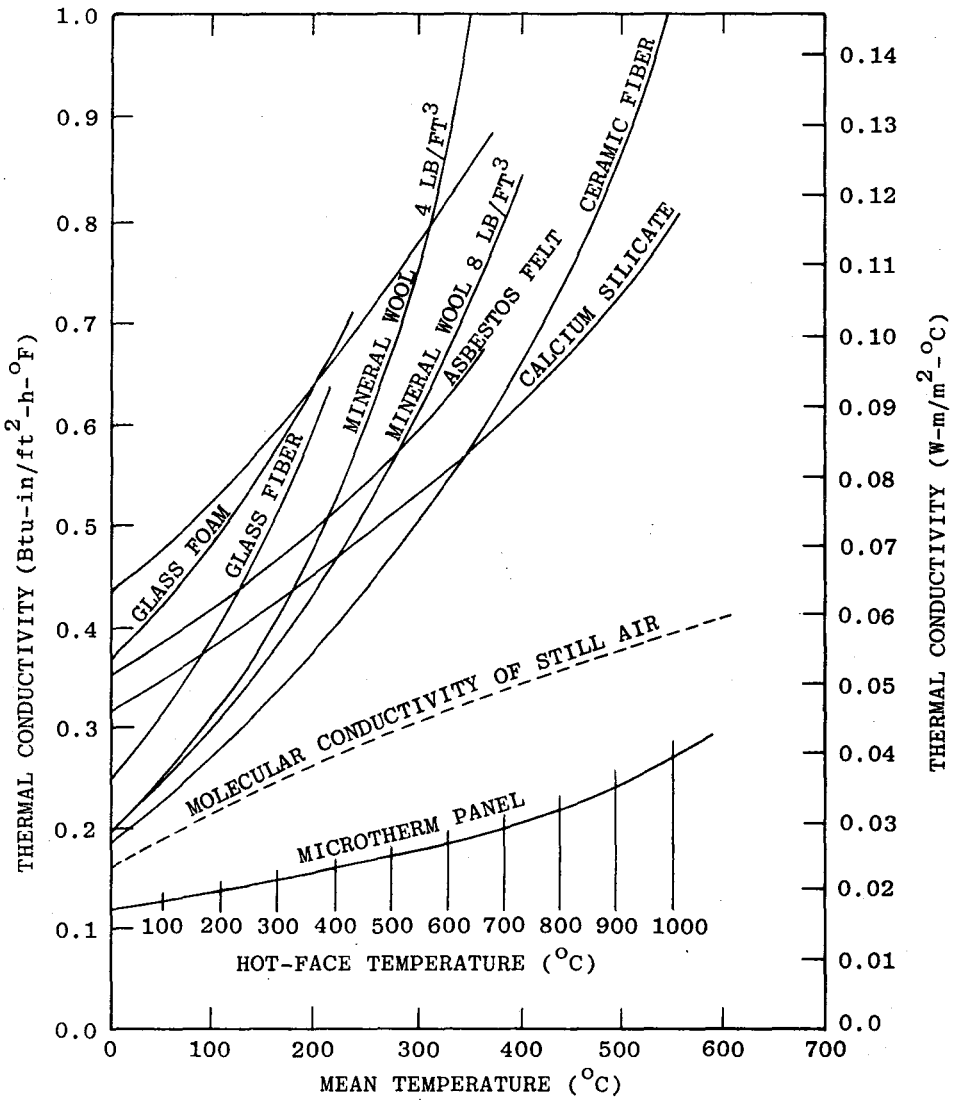

Figure 20. Thermal Conductivity Comparison of Different Insulation Materials.

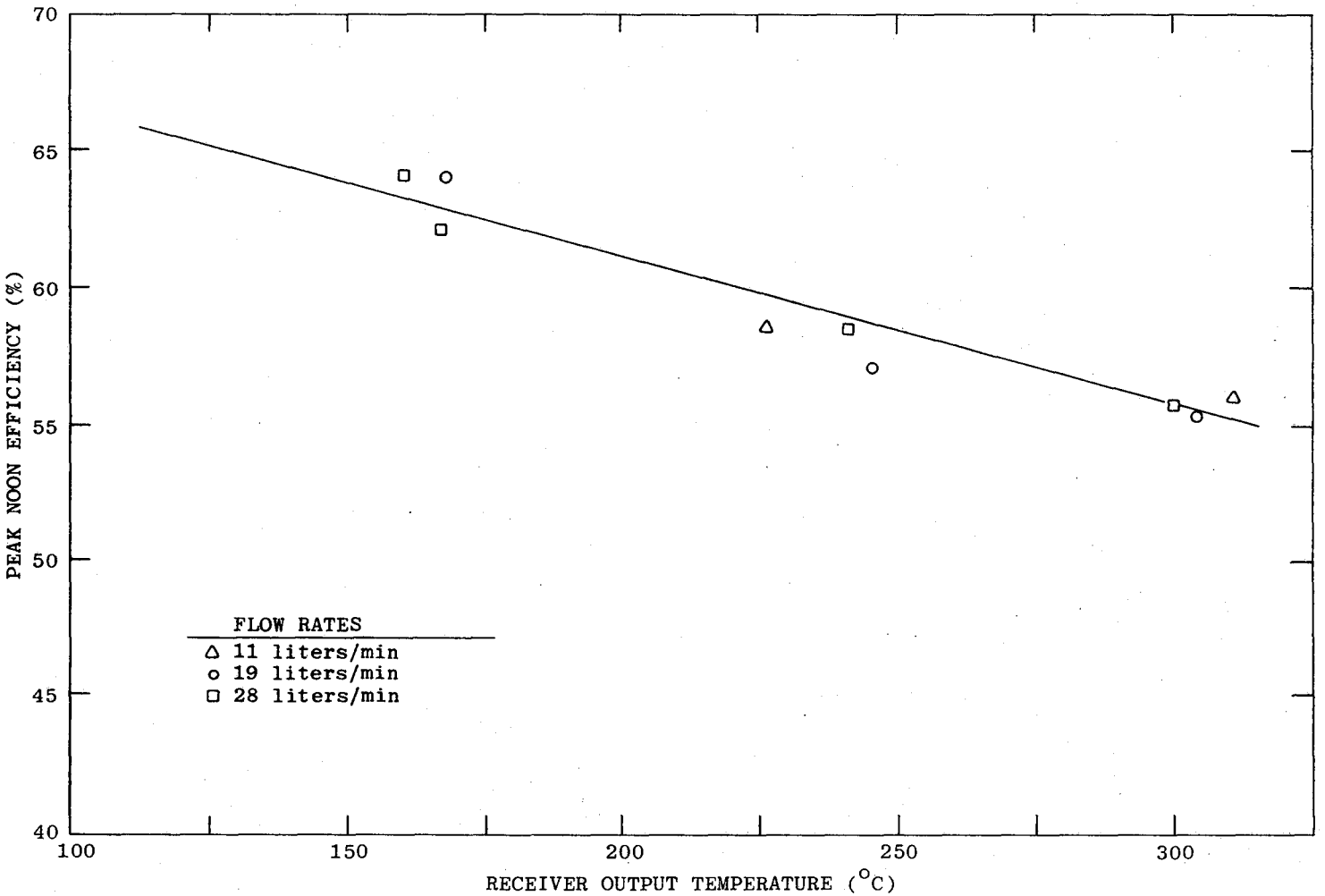

Figure 21. Hexcel Collector Efficiency vs. Output Temperature.

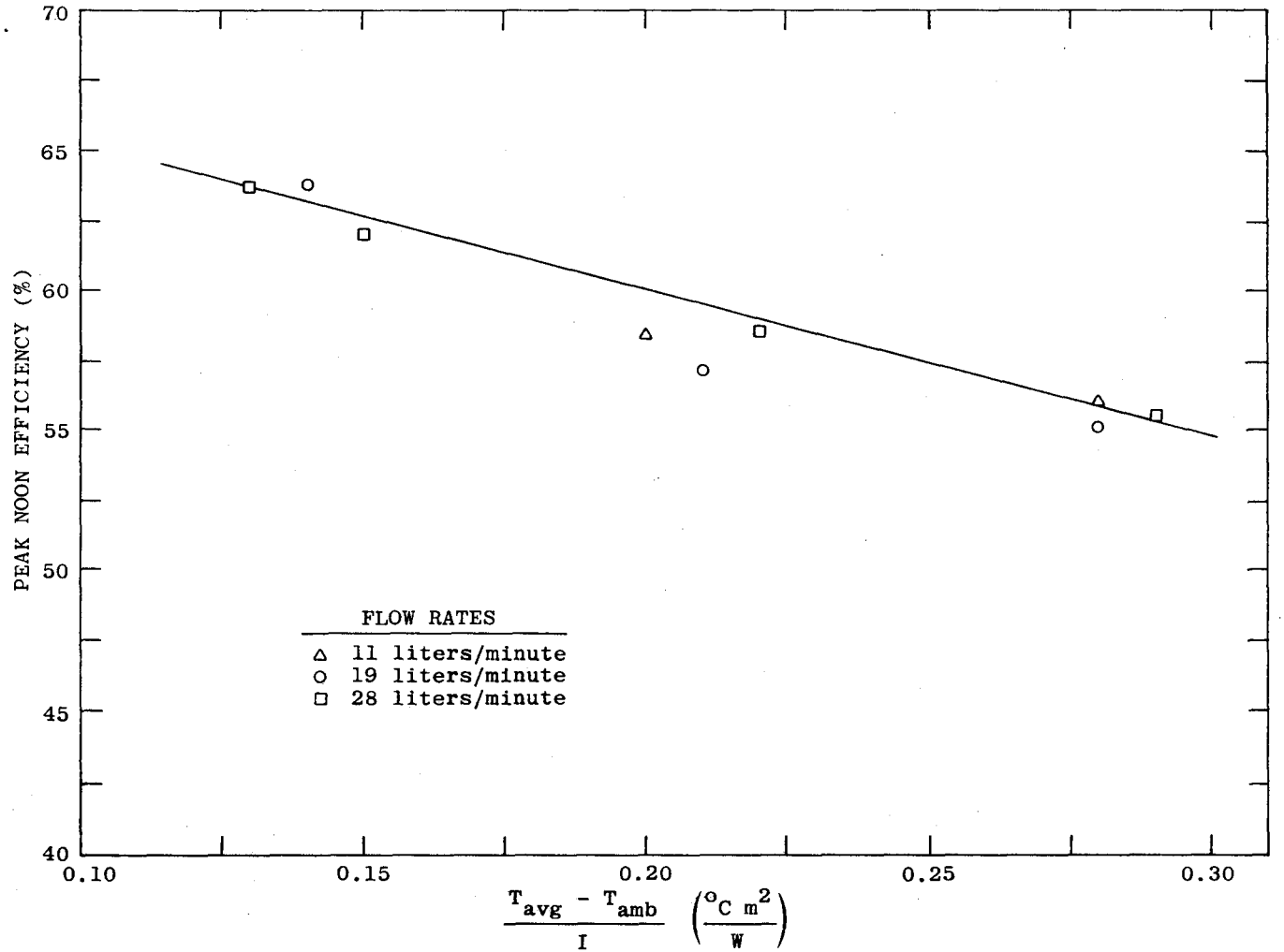

Figure 22. Hexcel Solar Noon Efficiency.

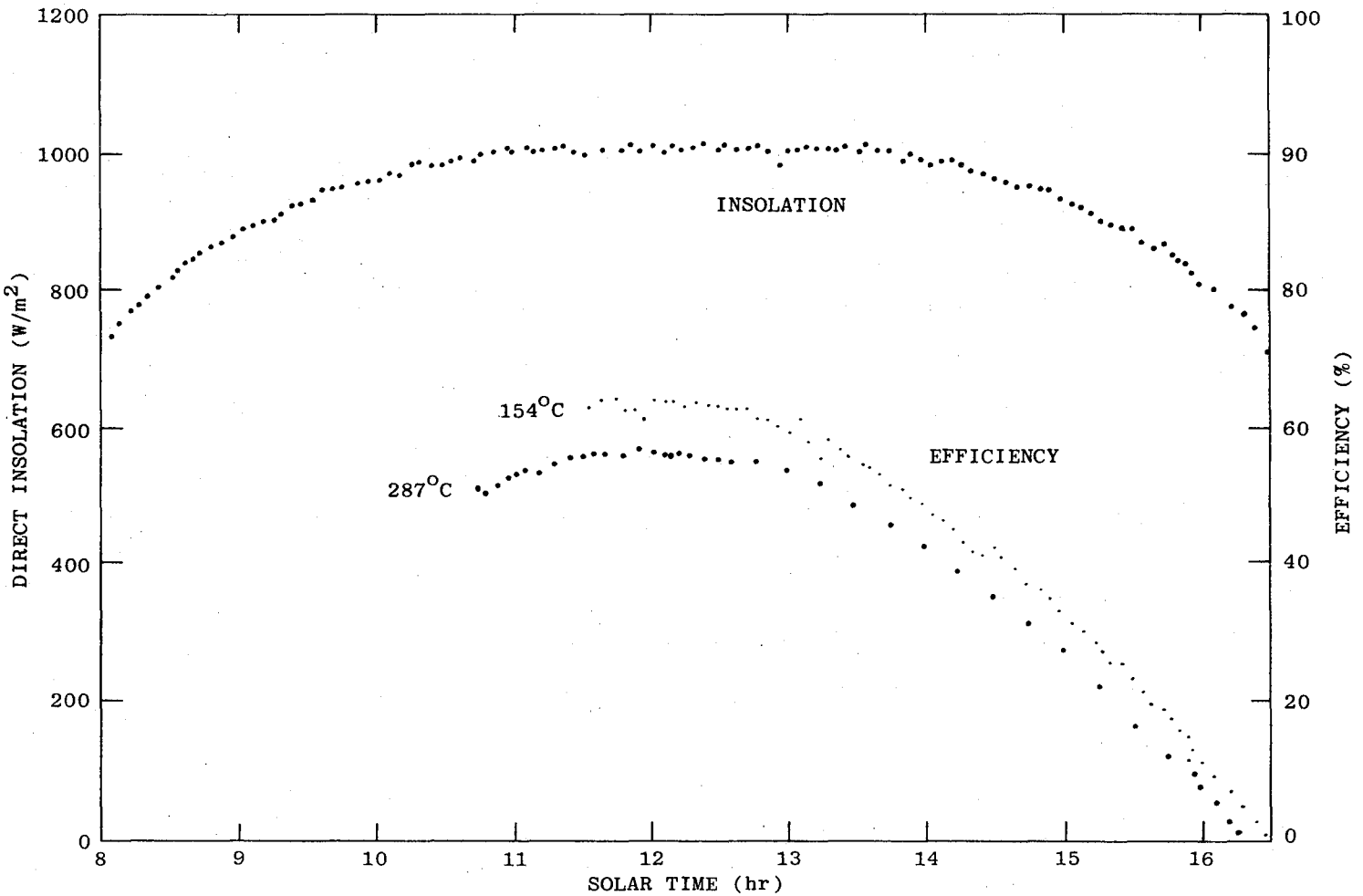

Figure 23. Hexcel All Day Efficiency.

causing the measured efficiency to be about 4% lower than would have been possible using an optimum black-chrome-coating with an absorptance of about 0.95. The Hexcel thermal loss is shown in Figure 24.

5.3 FMSC, GENERAL ATOMIC COMPANY

Figure 25 shows an efficiency curve obtained from the GA FMSC. Figure 26 is the same data plotted as a function of average receiver fluid temperature above ambient temperature divided by the direct insolation. The thermal efficiency performance of this collector fell well below predicted values. The difficulty was traced to inaccuracies in the reflective mirror surface, which caused the focal line to be too wide, spilling light outside the receiver aperture. This effect was documented by recording the reflected light intensity in a series of scans across the focal line at the receiver. Figure 27 is the result of several of these scans, showing that several mirror segments did not all focus their light in a band narrow enough to be captured within the receiver aperture. In Figure 27, Curve 2 would have fallen almost entirely within the aperture. The remaining curves have substantial portions falling outside the aperture. Overall, only about 71% of the light from the mirrors was captured by the receiver. Additional data on this problem can be found in Reference 11.

Preliminary measurements on a new FMSC module installed in the Systems Test Facility demonstrated a 90% capture of the reflected light. This should produce an efficiency of about 53% at 300°C, a notable improvement over the 42.5% measured on the test module at the CMTF.

Figure 28 shows thermal loss from the GA FMSC receiver. These losses are small --the loss per unit length of receiver is among the lowest measured at the CMTF. The exceptionally low conductivity of the Microtherm insulation used in the receiver (see Figure 20) and secondary concentration to a smaller active receiver area are believed responsible for the low loss. One loss measurement was made with the receiver window removed; as expected, this allows air conduction and convection to greatly increase the thermal loss.

5.4 FRESNEL LENS ROTATING ARRAY SOLAR COLLECTOR, McDONNELL DOUGLAS

Figure 29 shows the measured efficiency of the McDonnell Douglas linear Fresnel lens rotating array solar collector; Figure 30 shows same efficiency data plotted as a function of average receiver fluid temperature above ambient divided by direct insolation. In this case, this presentation of the efficiency data has increased the data scatter. Note that this collector did show some sensitivity of efficiency to the fluid flow rate. A slight redesign of the absorber tube could optimize this collector for lower flow rates if necessary in a systems design.

Figure 31 shows the performance of the McDonnell Douglas collector when operated at a constant temperature and flow rate throughout the day. The efficiency shown in Figure 31 is slightly lower than normal before 10:00 a.m. because the fluid system was still being heated, causing unstable, rising temperatures at the collector input. The measured efficiency increased about 4% at 10:15, when stabilized operating temperatures were established. The advantage of the fully tracking design is immediately apparent: the collector can operate at near peak efficiency for about 3 hours off solar noon, and falls only about 4% in efficiency at four hours off solar noon (an hour when the efficiency of an east-west trough collector is

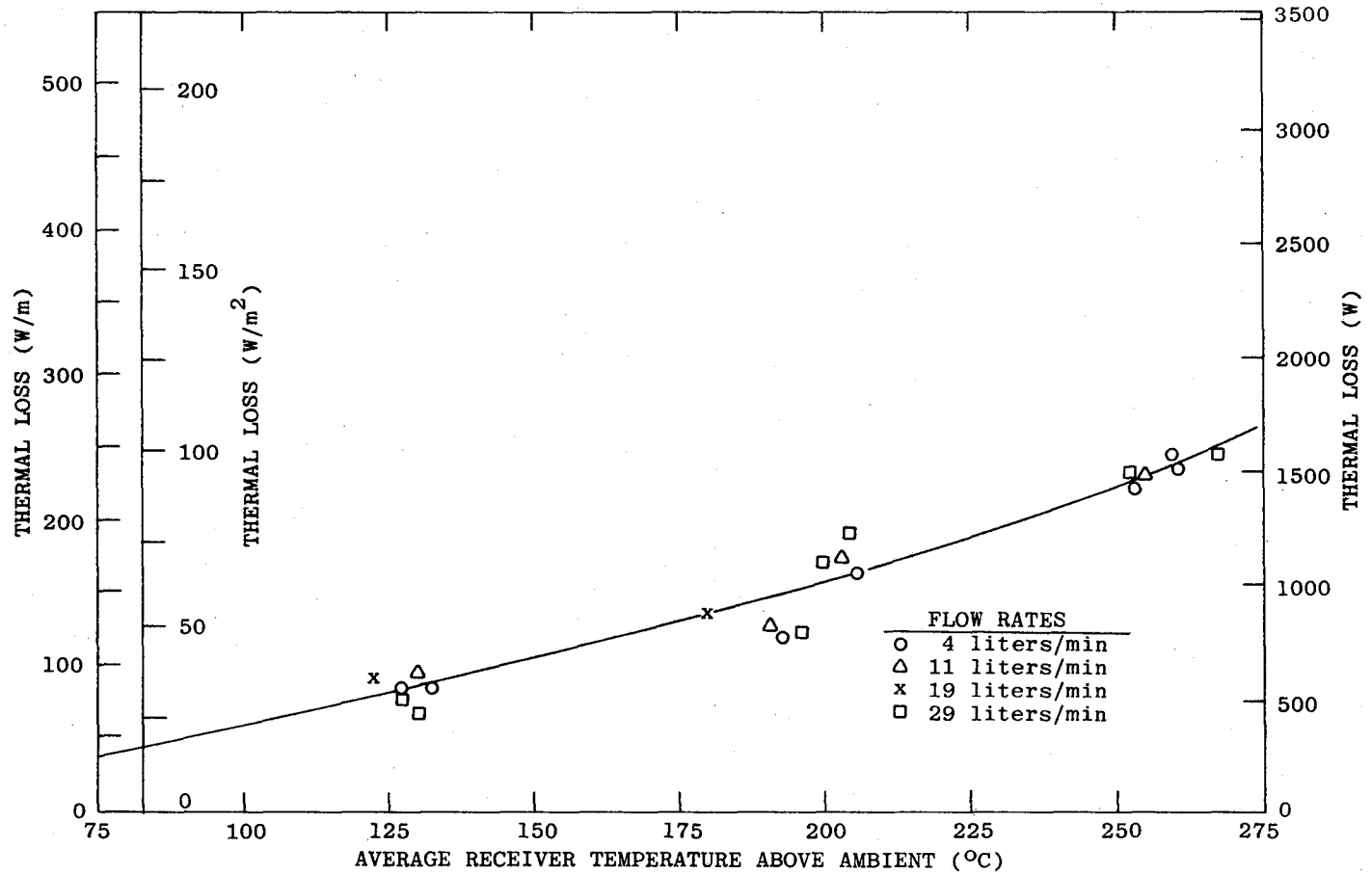

Figure 24. Hexcel Receiver Thermal Loss.

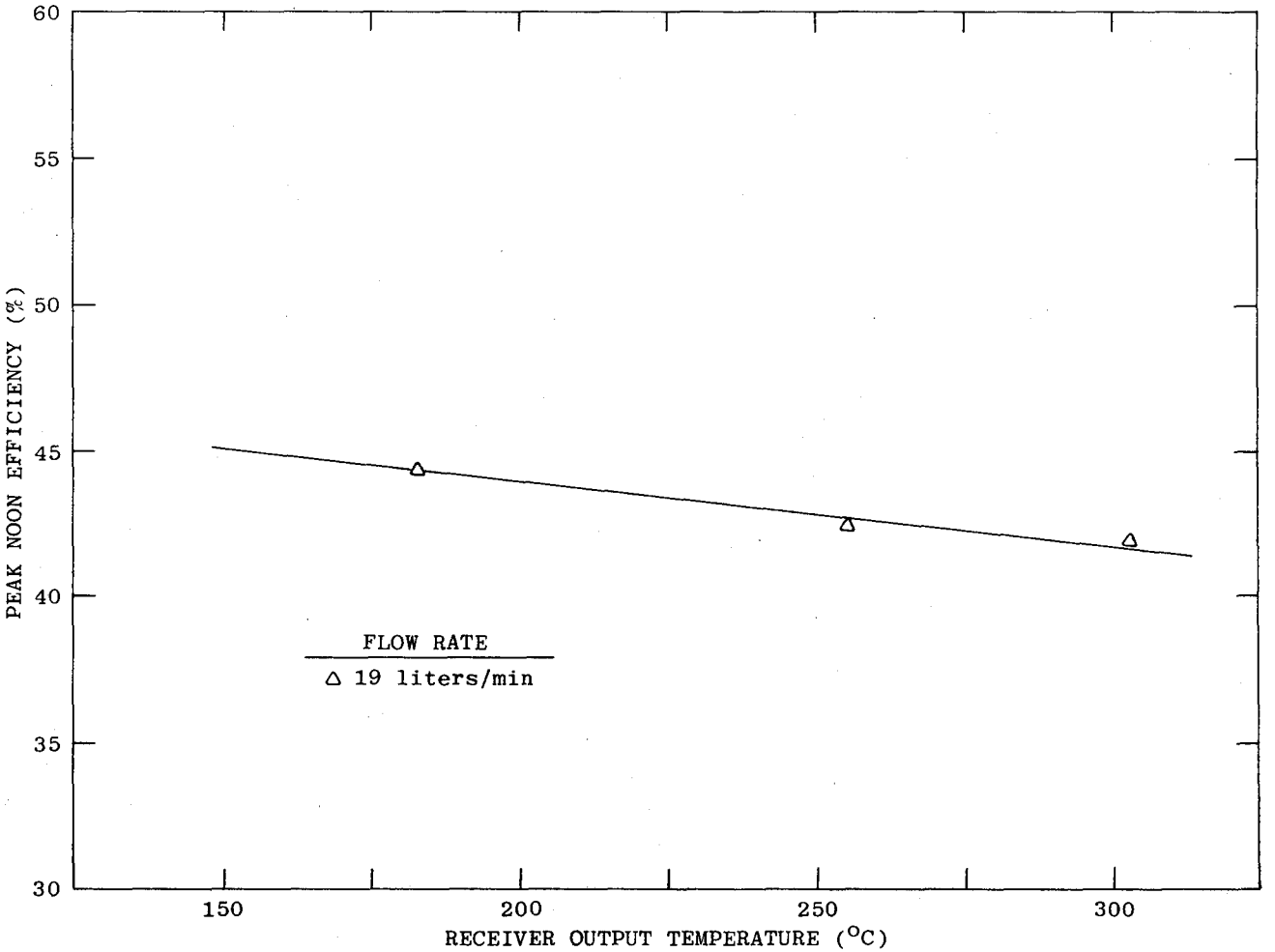

Figure 25. GA FMSC Efficiency vs. Output Temperature.

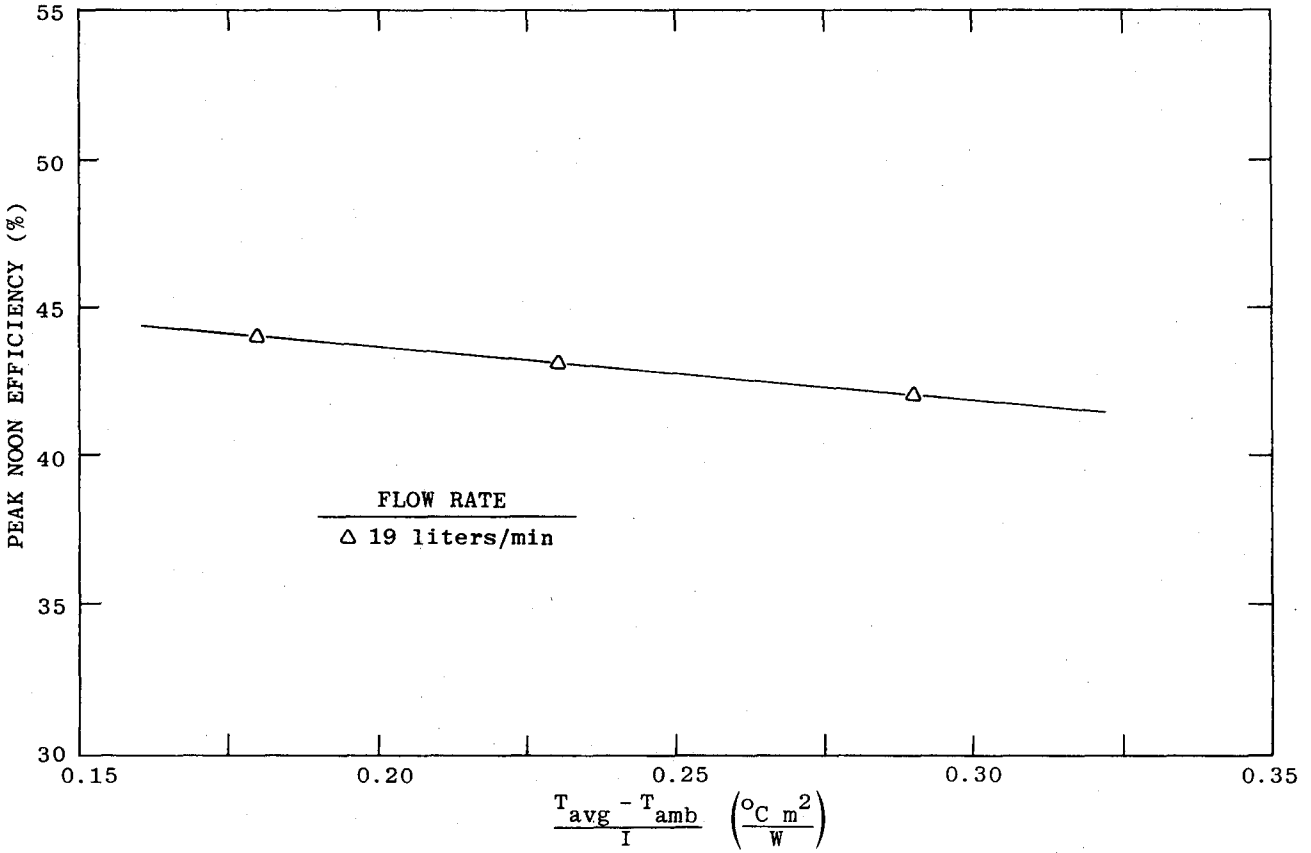

Figure 26. GA FMSC Solar Noon Efficiency.

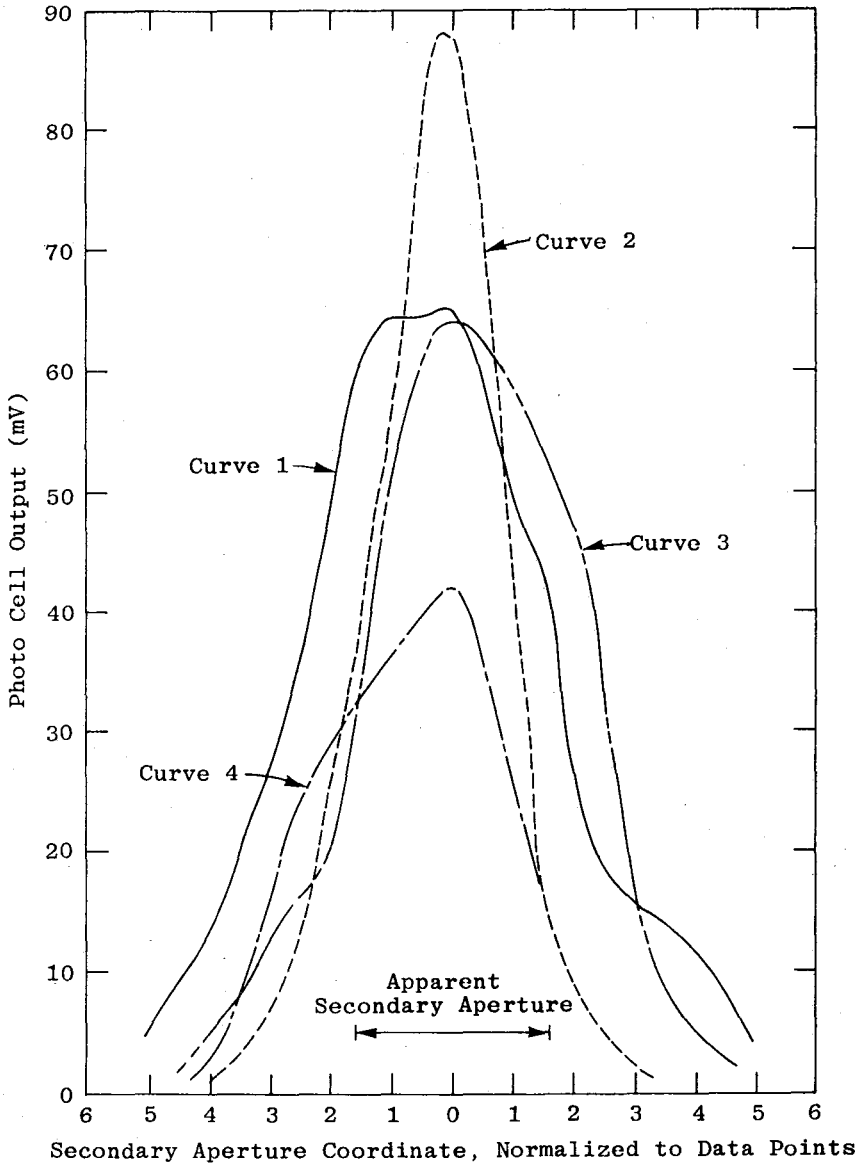

Figure 27. Light Intensity Scans Across FMSC Receiver Aperture.

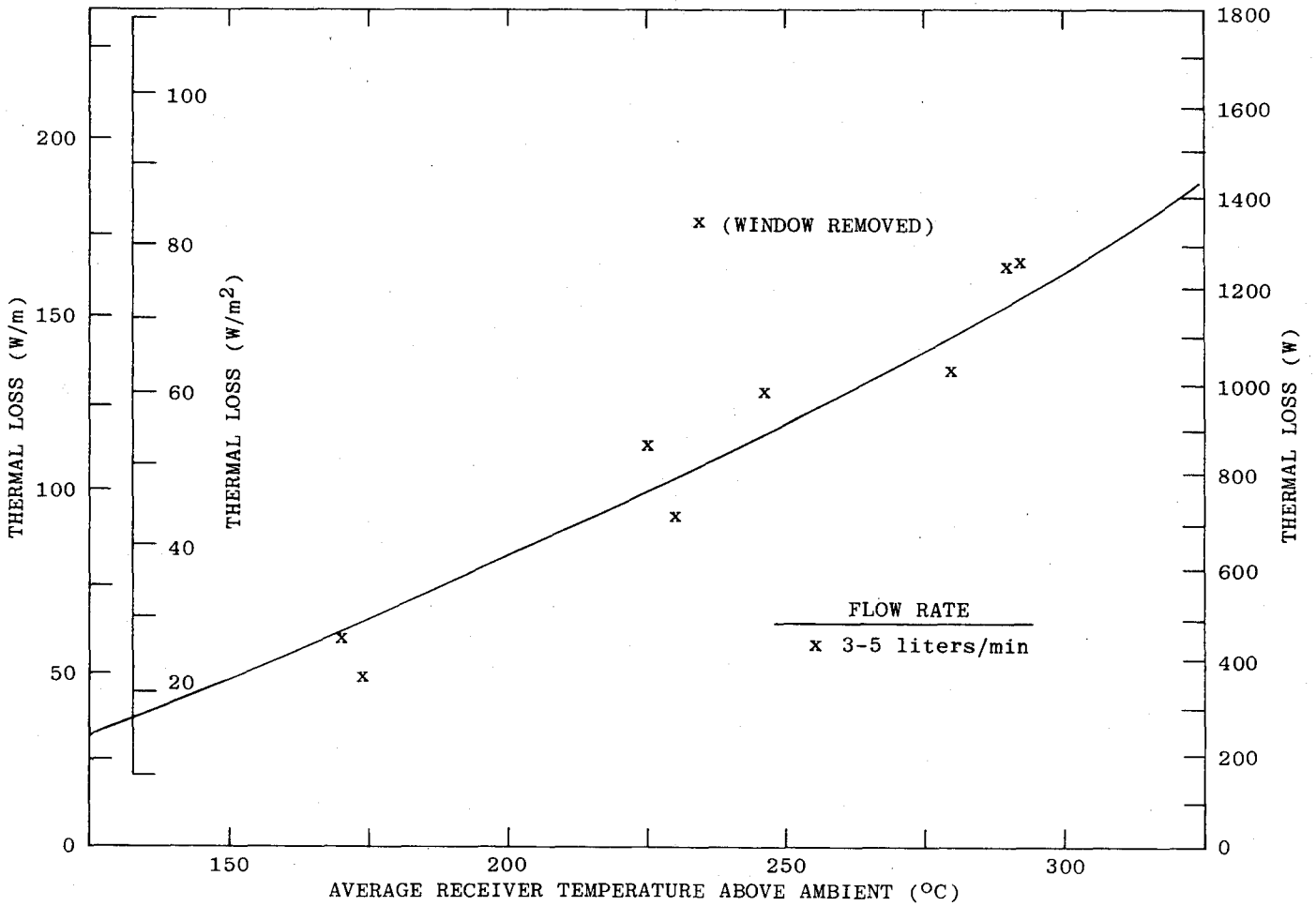

Figure 28. GA FMSC Receiver Thermal Loss.

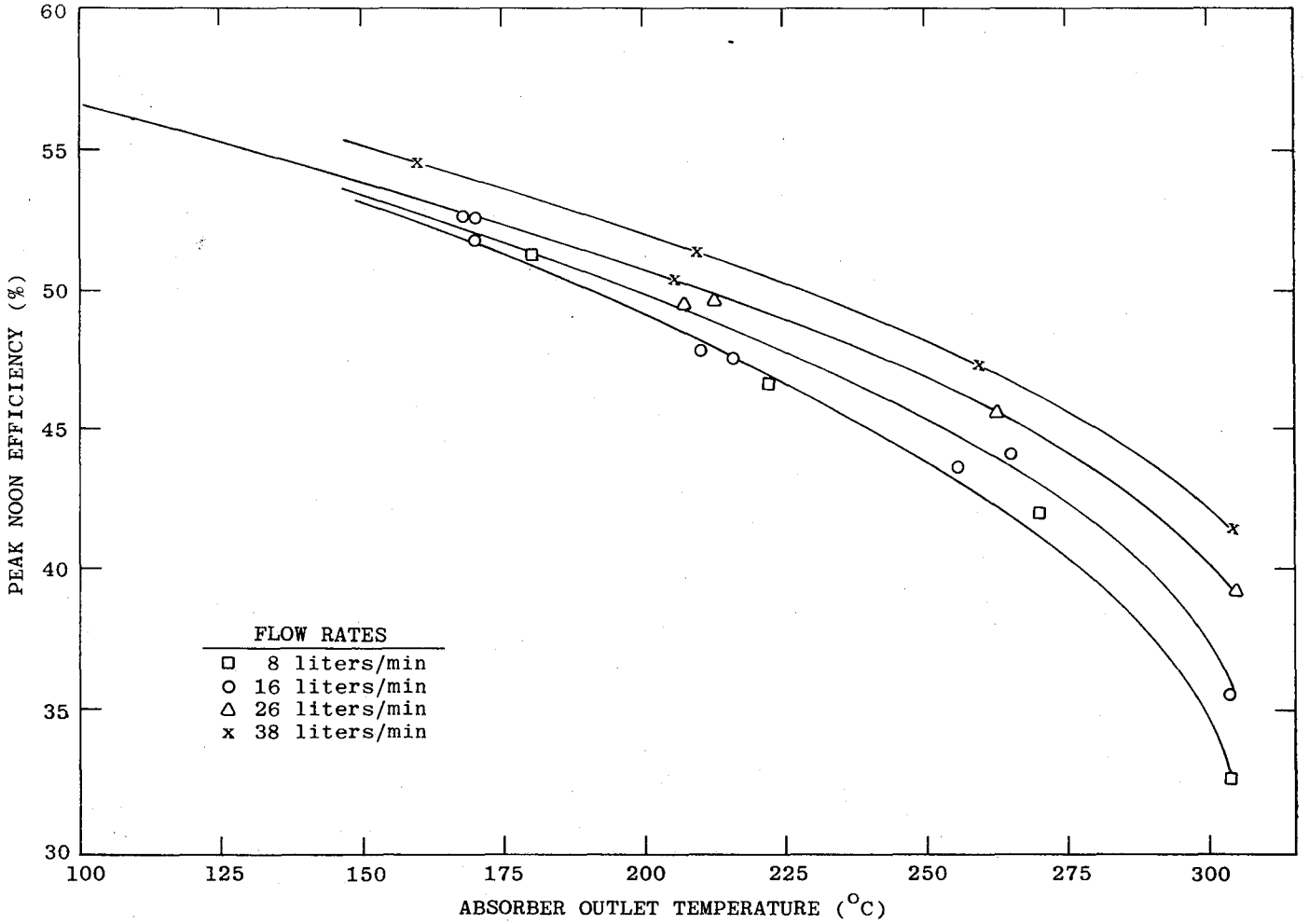

Figure 29. McDonnell Douglas Efficiency vs. Output Temperature.

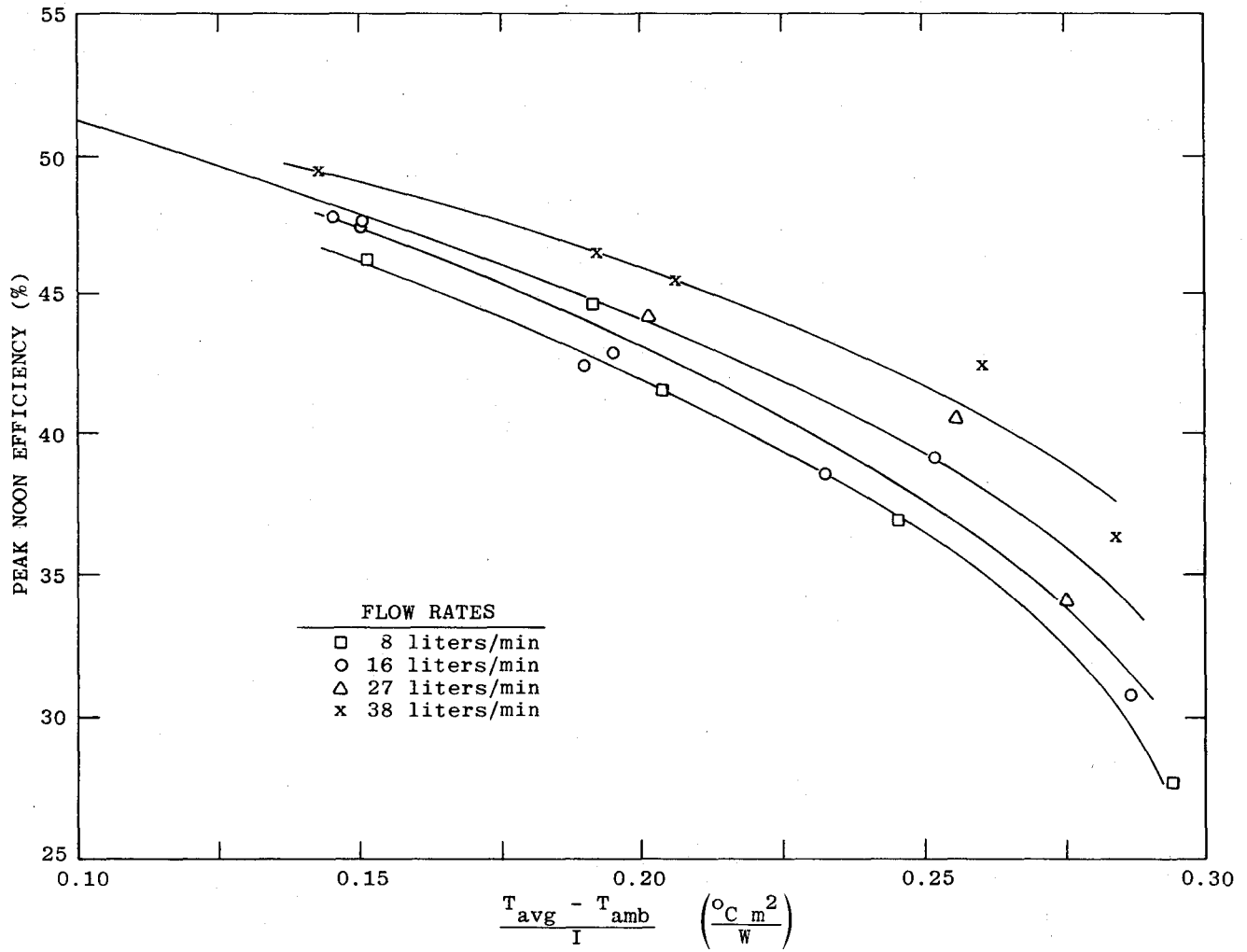

Figure 30. McDonnell Douglas Collector Solar Noon Efficiency.

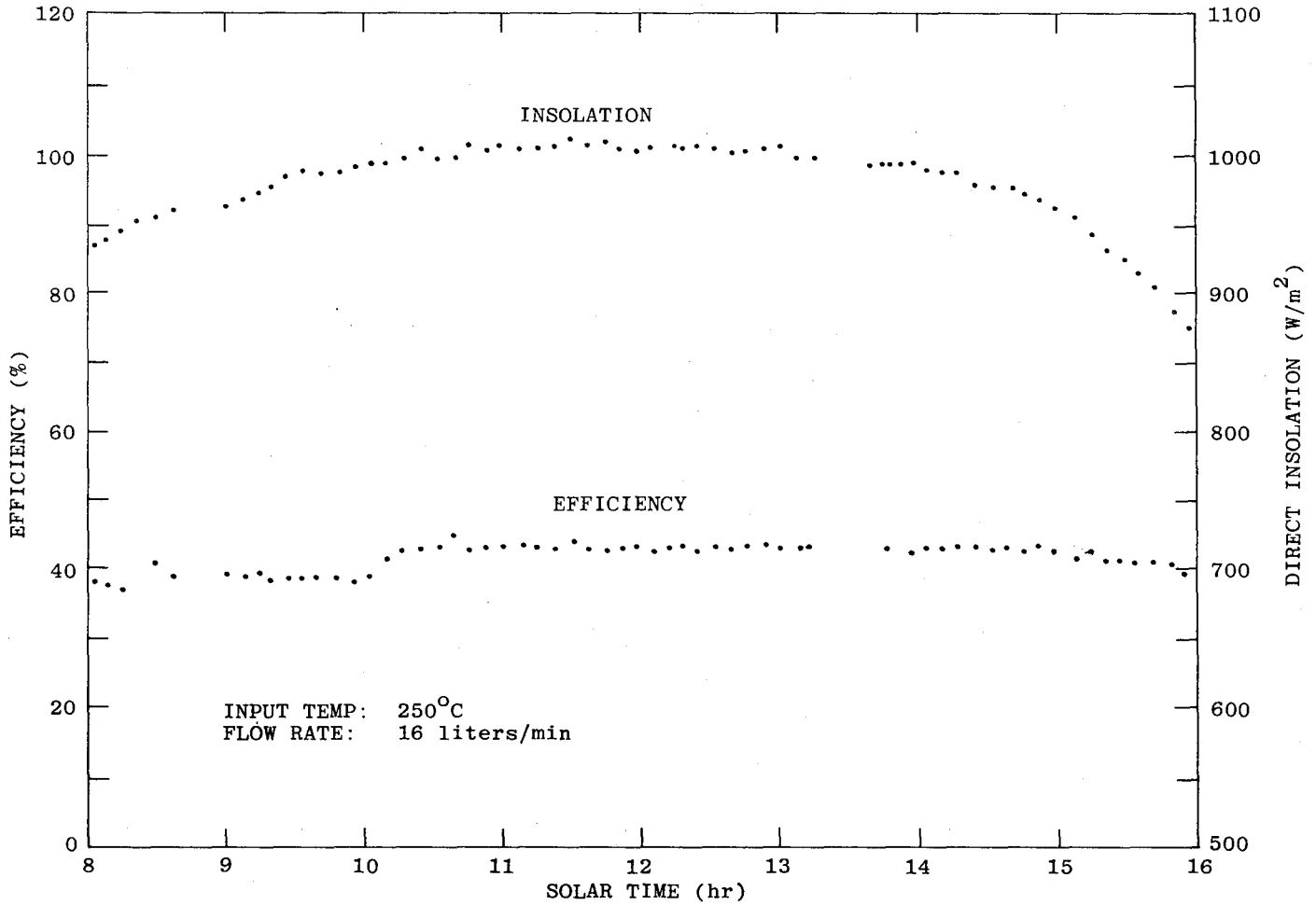

Figure 31. McDonnell Douglas All Day Efficiency at 250°C.

approaching zero). Over an 8-hour day such as the one shown in Figure 31, an energy recovery of about 11.2 MJ/m^2 could be obtained.

The measured efficiency of the McDonnell Douglas collector did not reach pretest expectations. The primary reason for the lower efficiency was probably the transmission characteristics of the cast-acrylic Fresnel lenses. They had a solar spectrum transmissivity of only about 70%, compared to the 80% obtainable through an optimum piece of acrylic. Another factor may have been alignment of the absorber tube with the focal line. During the test, one of the absorber tubes was observed to be slightly offset from the focal line over part of its length. The misalignment was not corrected, and the loss of efficiency from this cause is not presently known.

Extensive data was recorded on magnetic tape during the tests on the McDonnell Douglas collector. Included in this recorded data are efficiency measurements on two of the four individual absorbers inside the collector; data has not yet been analyzed to determine any differences between the four sections that would make the total collector efficiencies quoted here not representative of the collector's real capability. Further information should be available soon.

Figure 32 shows the thermal losses measured on the McDonnell Douglas collector, shown in watts (W), W/linear meter of heated pipe within the collector, and W/m^2 of collector aperture area.

5.5 LINEAR PARABOLIC TROUGH CONCENTRATOR, SOLAR KINETICS, INC.

Figure 33 is the result of efficiency testing on one 12.2 m length of Solar Kinetics linear parabolic trough collector. Figure 34 presents the same efficiency data as a function of average receiver fluid temperature above ambient temperature divided by direct insolation. The maximum efficiency achieved was not as high as had been predicted; the reason was traced to a manufacturing problem. The bulkheads used to provide the parabolic shape to the monocoque construction are normally a one-piece precision aluminum casting. These castings were not available in the full aperture width when the test collector was being assembled, so a shorter casting was used. An aluminum extrusion about 15 cm wide was then used on each side to fill out the full aperture width. The parabolic surface from the casting-extrusion interface outward was not sufficiently precise, causing considerable reflected light to miss the receiver.

An experiment was conducted to attempt a definition of the problem. The outer 15 cm of each side of the mirror was masked with black plastic and efficiency was measured; the measurement was then repeated with the mask removed. Calculations indicate that the mirror center has an optical efficiency of about 90%, while the outer 15 cm has a much lower optical efficiency, about 75%. The design tested to date is not representative of normal construction. Negotiations are under way with the builder to obtain a new mirror assembly, which would be constructed with one-piece castings. The new mirror should exhibit improved performance.

Figure 35 was obtained from two all-day tests at a constant input temperature and flow rate. The upper curve represents an input temperature of 150°C; the flow rate was changed from 19 liters/min to 38 liters/min at mid-day. No significant change in efficiency was found. The "glitches" in the curves resulted from slight problems with sun tracking equipment.

The lower curve in Figure 35 was the result of an input temperature of 250°C. From 8 a.m. to 4 p.m., about 11.5 MJ/m^2 could be obtained from this collector at

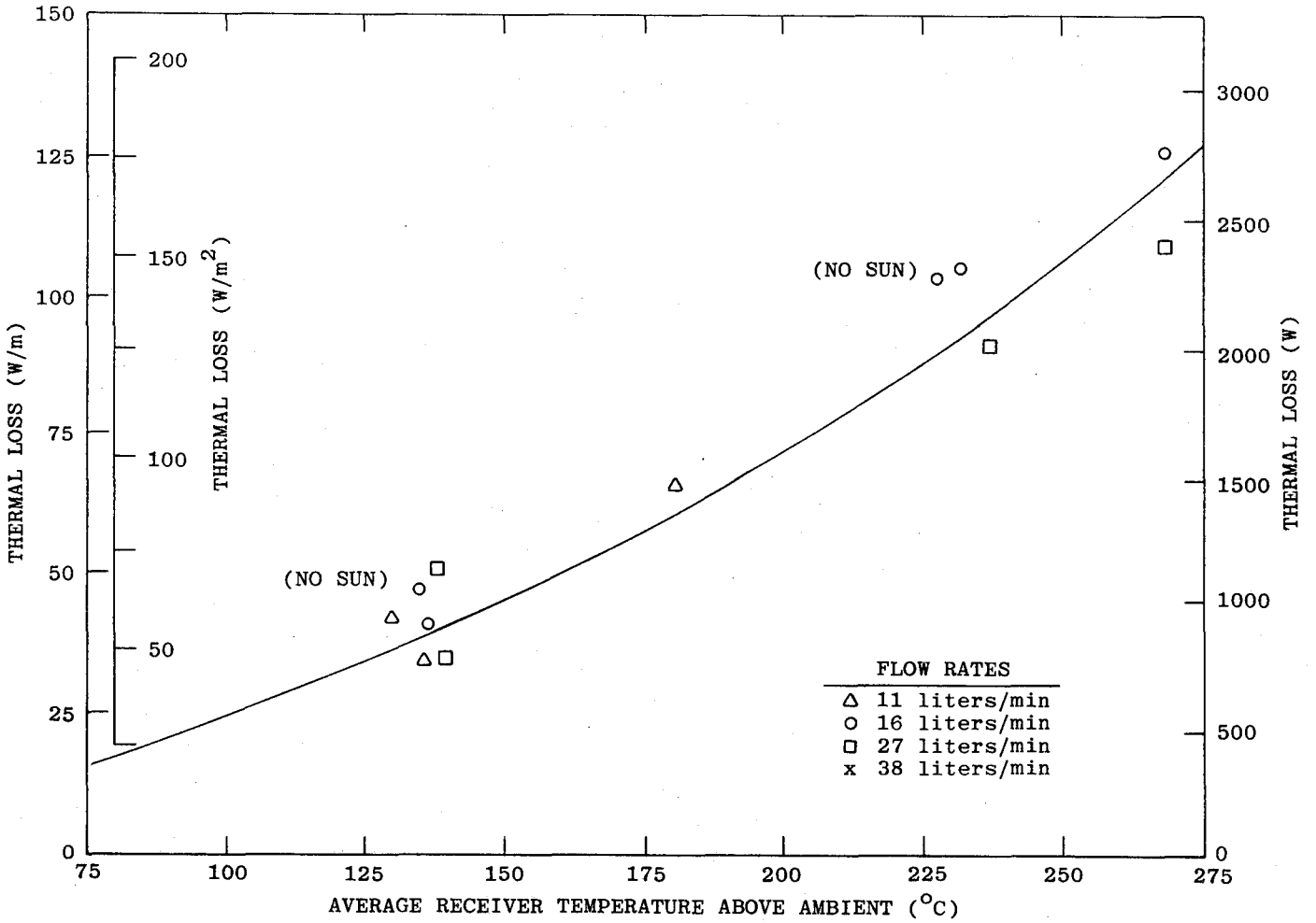

Figure 32. McDonnell Douglas Receiver Thermal Loss.

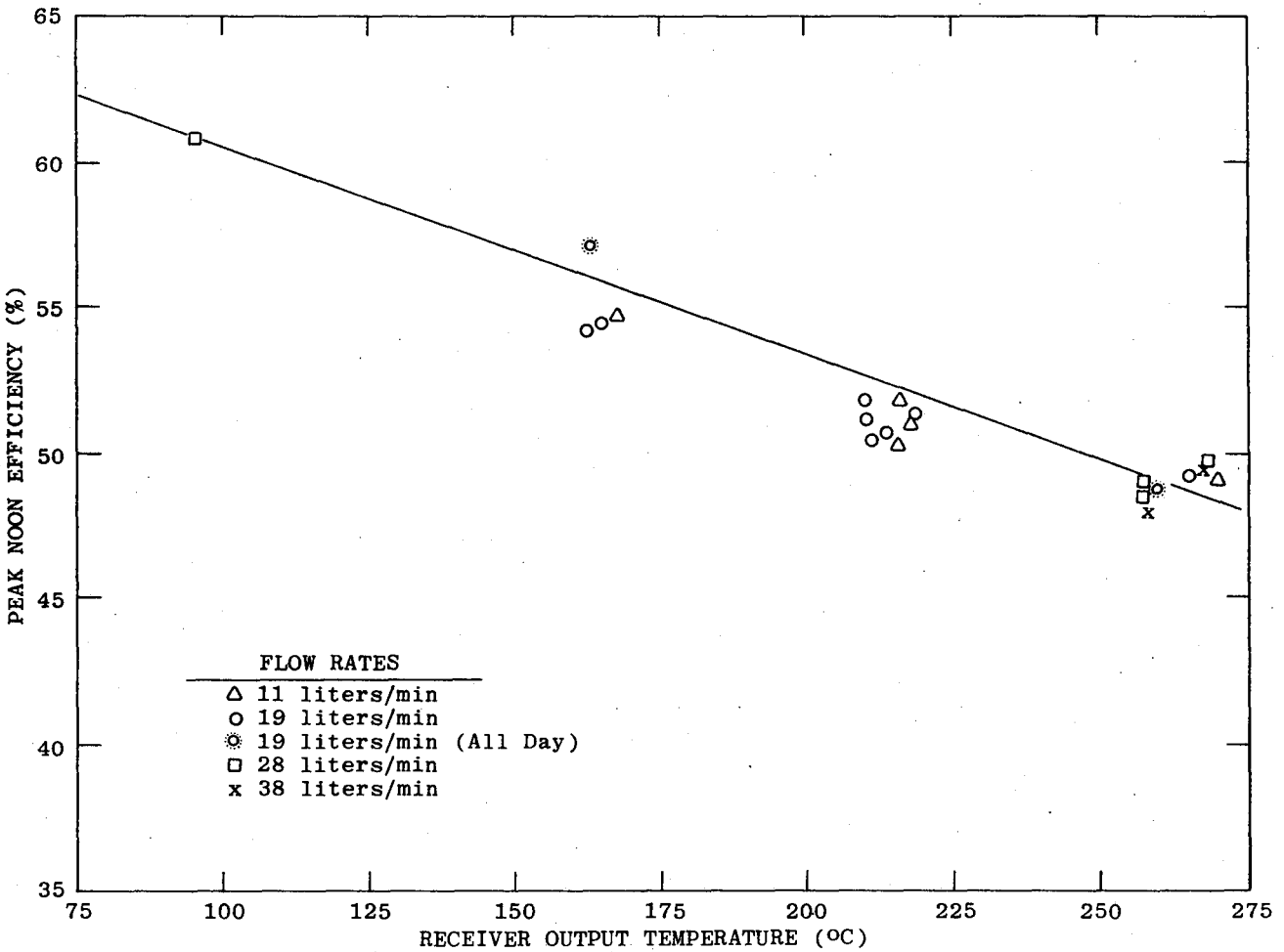

Figure 33. Solar Kinetics Efficiency vs. Output Temperature.

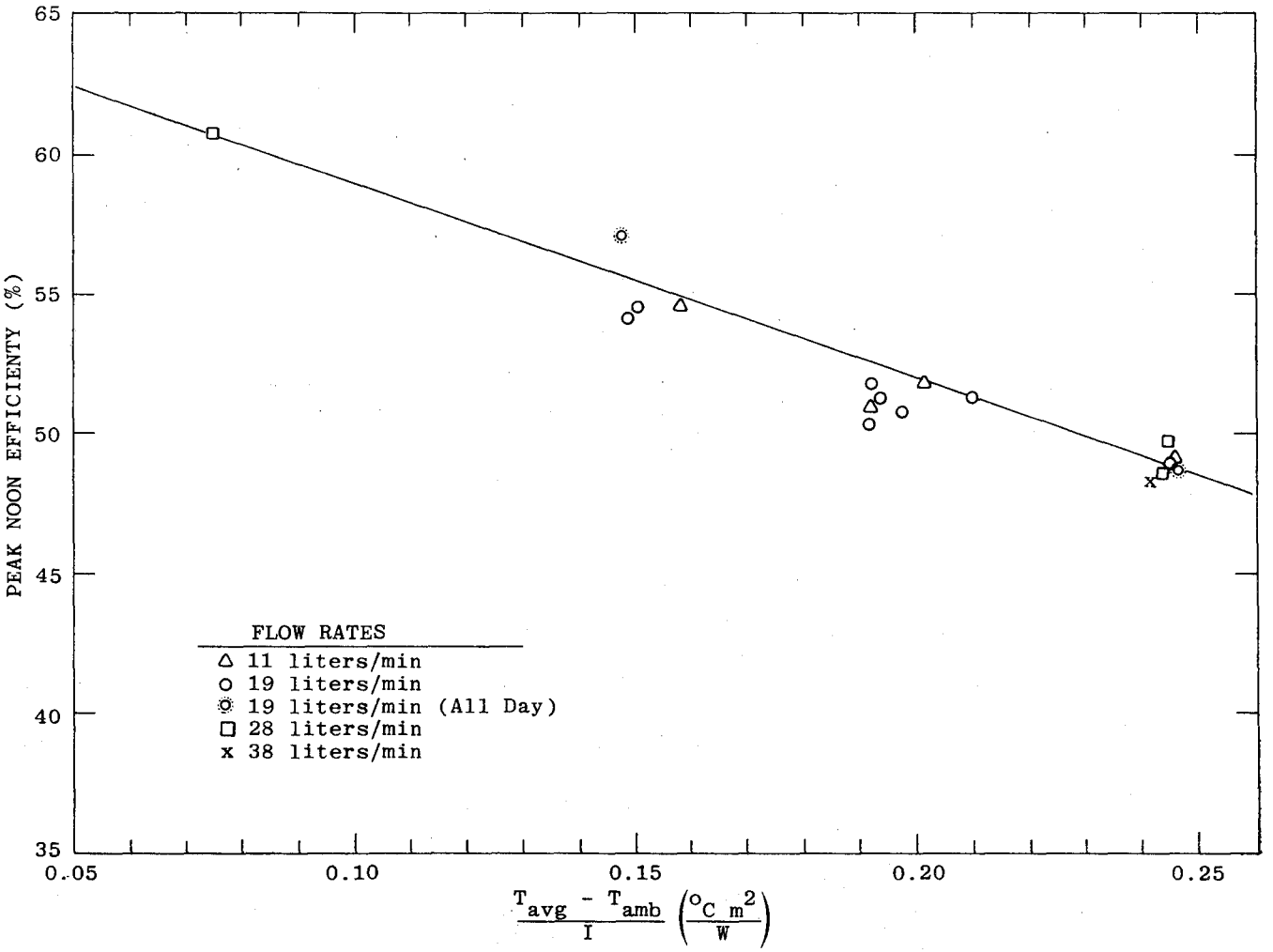

Figure 34. Solar Kinetics Collector Solar Noon Efficiency.

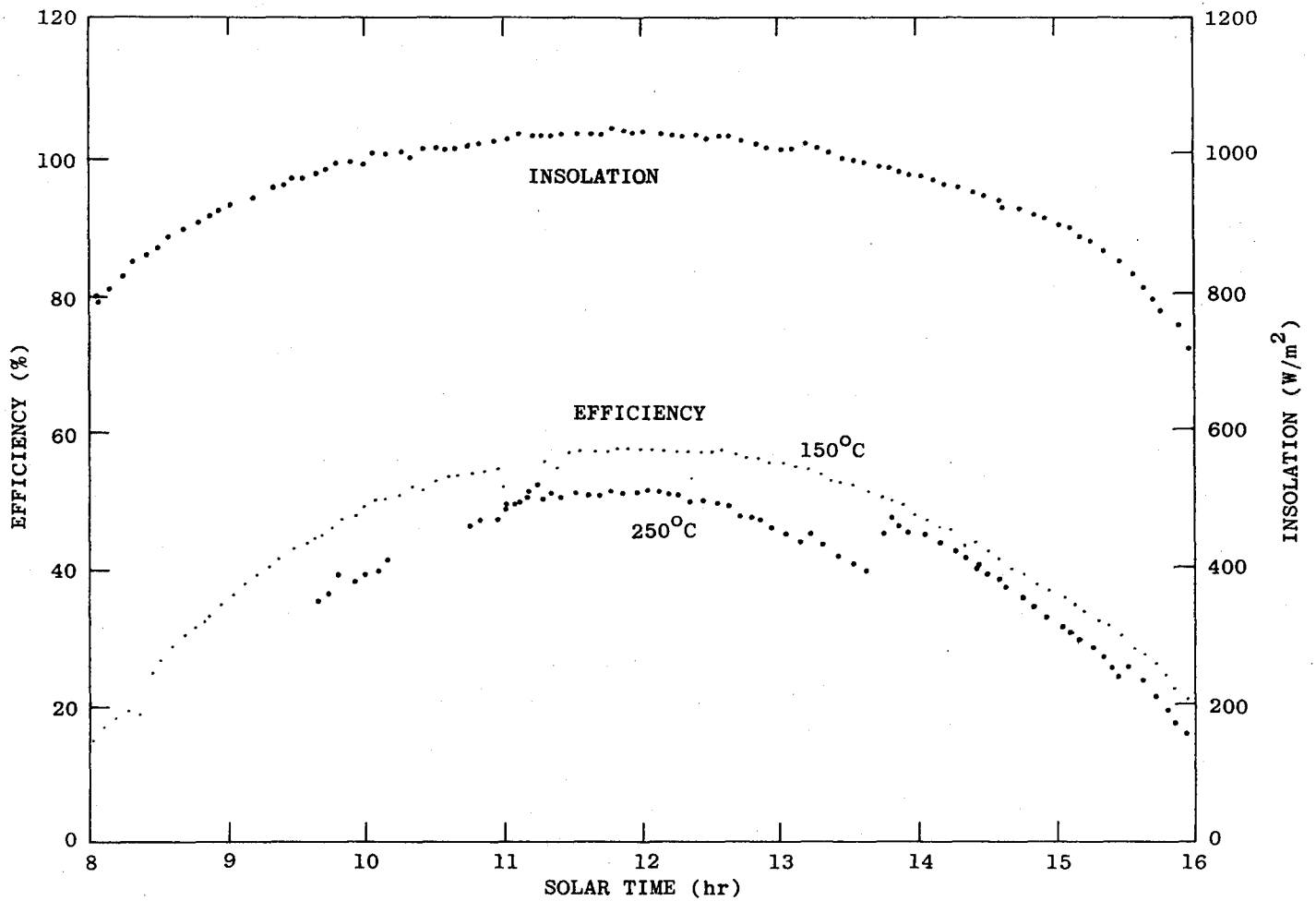

Figure 35. Solar Kinetics All Day Efficiency.

150°C, or about 8.9 MJ/m^2 at 250°C. As with other east-west oriented trough collectors, less end spill-off would occur when the Solar Kinetics collectors are placed in long rows in a large field, so somewhat larger amounts of energy per square-meter would be available than are indicated by our test results.

Because of temperature limitations on Teflon spacers and hoses, the Solar Kinetics collector tested was limited to an output temperature of about 287°C. The other collectors were all tested to output temperatures around 315°C. An output temperature of 287°C is not a fundamental limitation of the Solar Kinetics collector, since simple replacement of the Teflon parts allows operation at higher temperatures.

Figure 36 is the result of thermal loss testing on the Solar Kinetics collector. These losses are quite low. Analysis of loss data on the collector is not complete --Figure 36 is based on only a small number of loss points taken with air in the annulus space between absorber tube and the glass cover. Preliminary data indicate even lower losses are possible if argon or a vacuum replace air in the annulus space. Further information may be obtained from Reference 13.

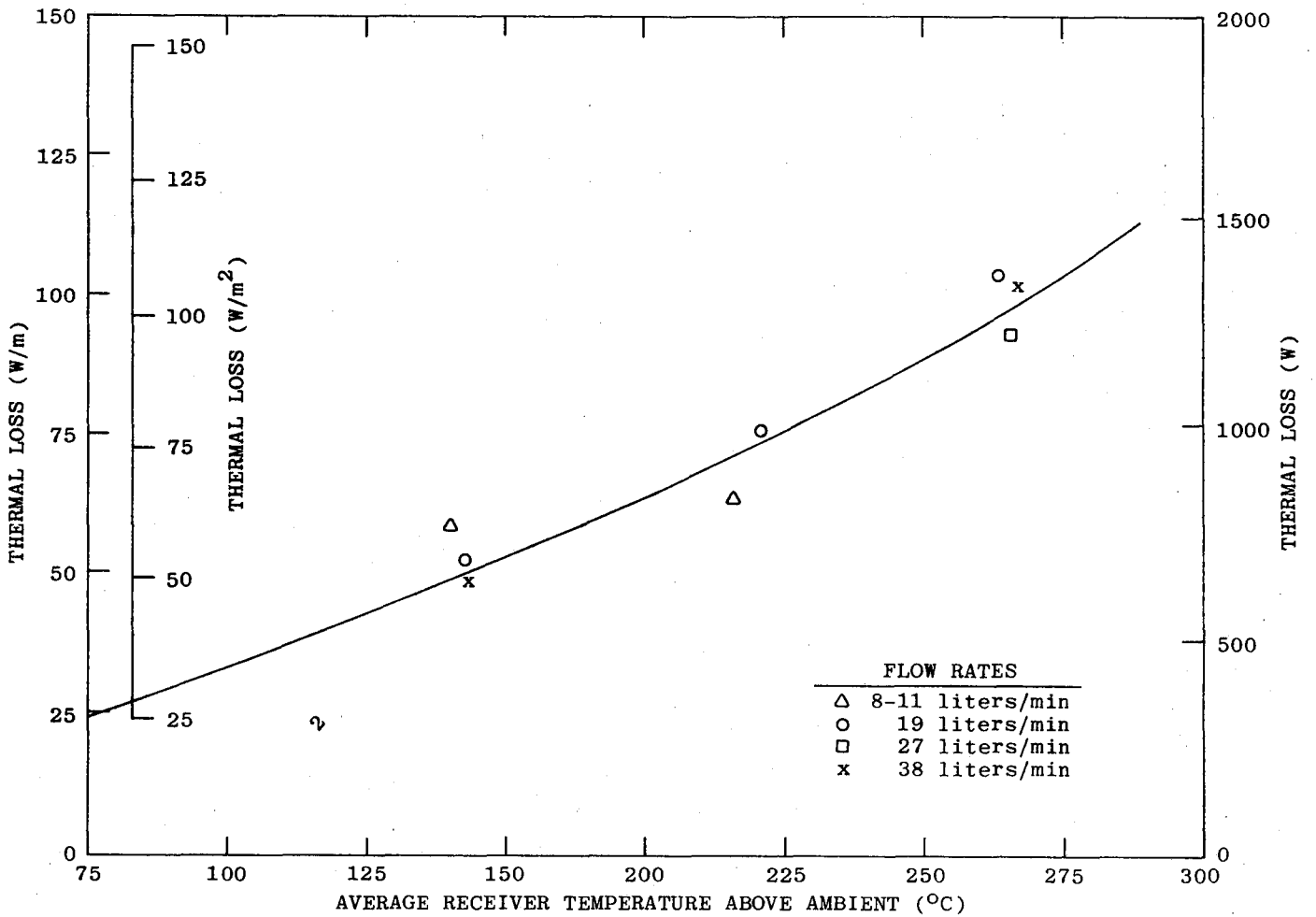

Figure 36. Solar Kinetics Receiver Thermal Loss.

6. CONCLUSIONS

Figures 37 and 38 show efficiency plots for all the collectors. The Hexcel design performed better than the others, primarily for one reason: a highly reflective, precisely shaped mirror that focused almost all the reflected light onto the absorber.

The McDonnell Douglas, Suntec Systems, and Solar Kinetics designs were down about 10% in efficiency at temperatures around 300°C; these three exhibited essentially similar thermal efficiency performance.

The General Atomic FMSC performed at a lower level at low temperatures, due to large reflected light spillover. However, because of very low thermal losses, the FMSC thermal efficiency performance was only about 3 to 4% lower than the others near operating temperatures of 300°C.

The magnitude of actual thermal loss cannot be directly compared between the various collectors; they differ too widely in size and design concept. It is difficult to find a loss parameter for normalization of all designs in the same sense as an efficiency comparison. When compared on the basis of loss per linear foot of receiver, those with small receivers, such as Solar Kinetics, and those with buried, well-insulated absorbers, such as GA and McDonnell Douglas, exhibit the lowest losses. This comparision may be unfair to a system such as the Suntec SLATS, which by virtue of its design concept must use a relatively large, wide receiver assembly.

Another comparison of losses that can be made is loss per unit of collector aperture. This method tends to penalize low-concentration-ratio collectors such as Solar Kinetics and McDonnell Douglas, over a high-concentration-ratio system such as that of Hexcel.

Figures 39 and 40 compare thermal loss for both loss per unit area and loss per unit length of receiver. These and many other characteristics must be considered in a decision as to which would be best suited for a given application.

From all the problems encountered with these collectors during their test series, the technological immaturity of solar collector designs is apparent. Even the best can be significantly improved. Most of the design, manufacture, and operational problems encountered with all the collectors tested appear to be easily correctable, leading to substantial gains in efficiency, especially for those on the lower end of the efficiency scale.

Though not outlined in this report, the testing apparatus caused almost as many operating problems as the tested devices. Lessons learned here also have applications in preventing problems and improving reliability of future operational solar thermal systems.

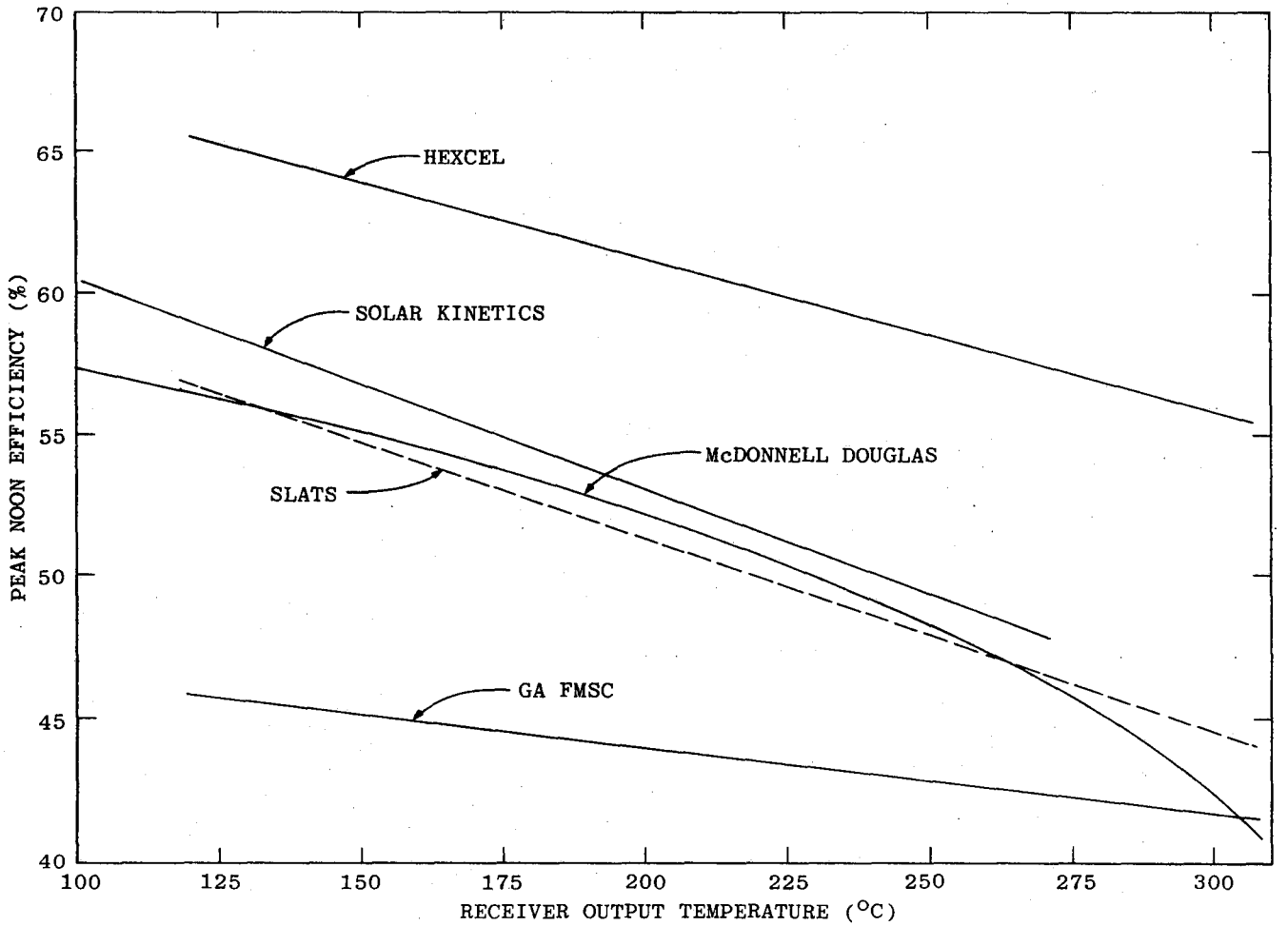

Figure 37. Comparison of Efficiency vs. Output Temperature.

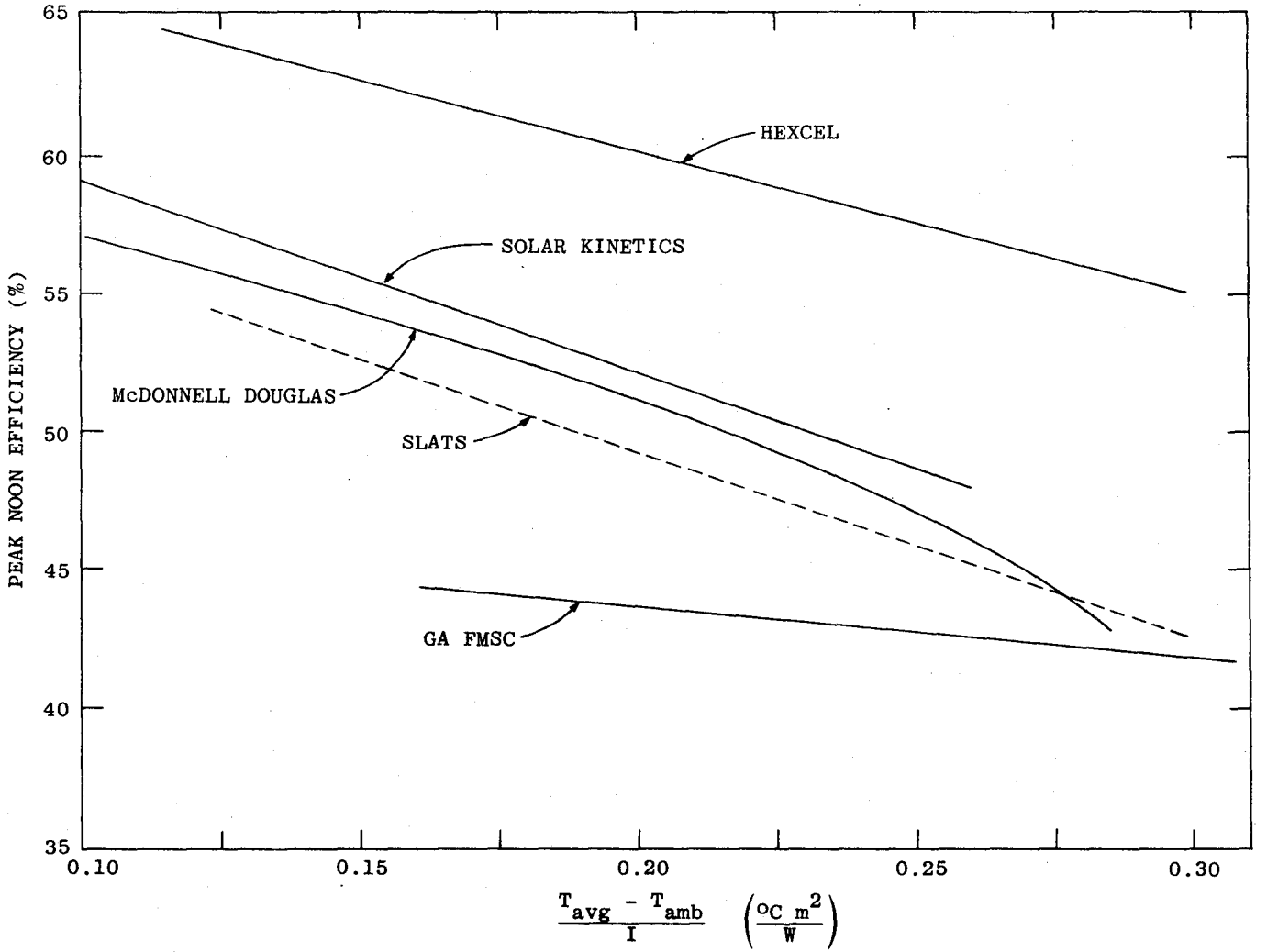

Figure 38. Comparison of Solar Noon Efficiency.

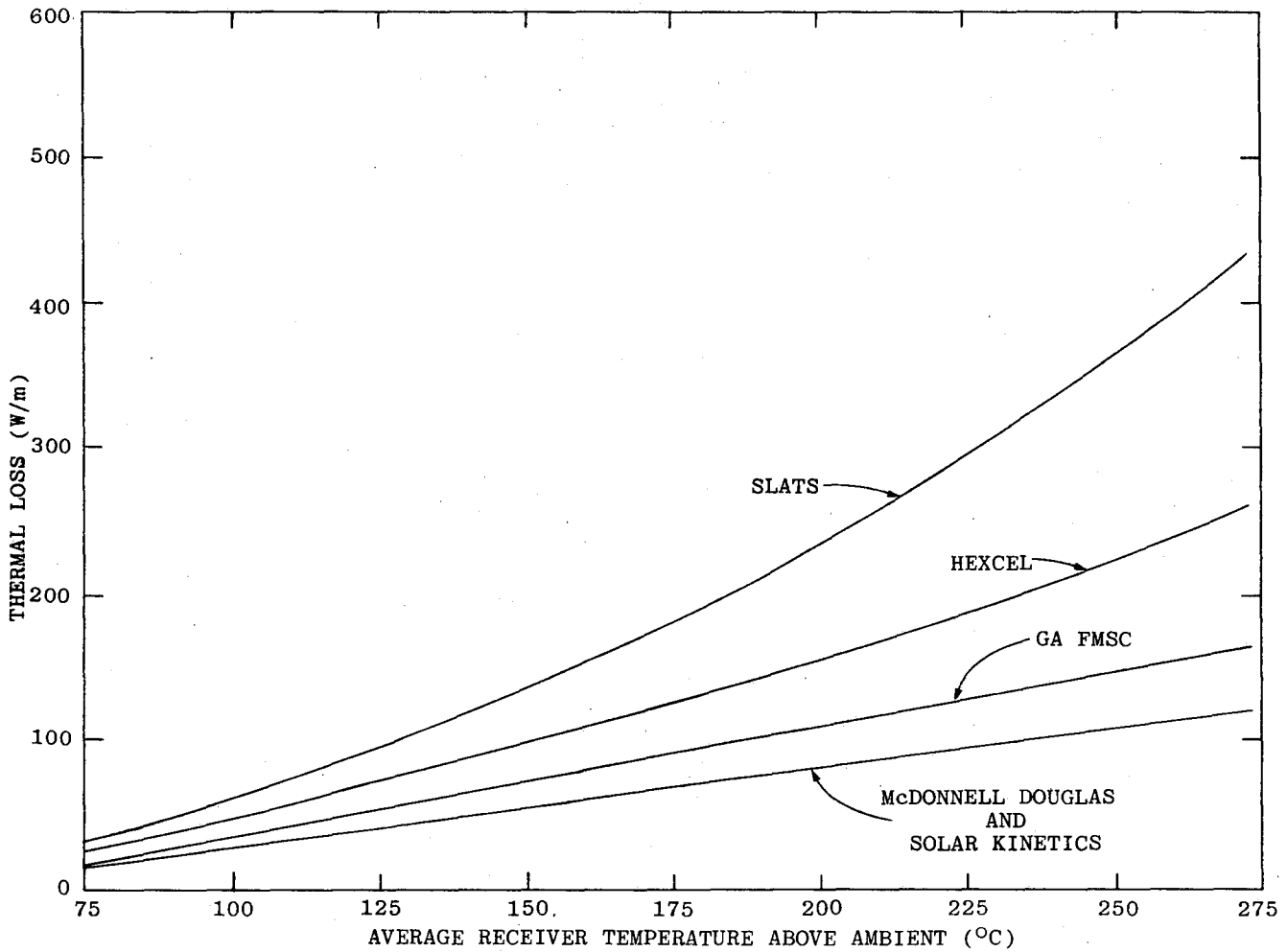

Figure 39. Comparison of Thermal Loss Per Meter of Receiver Length.

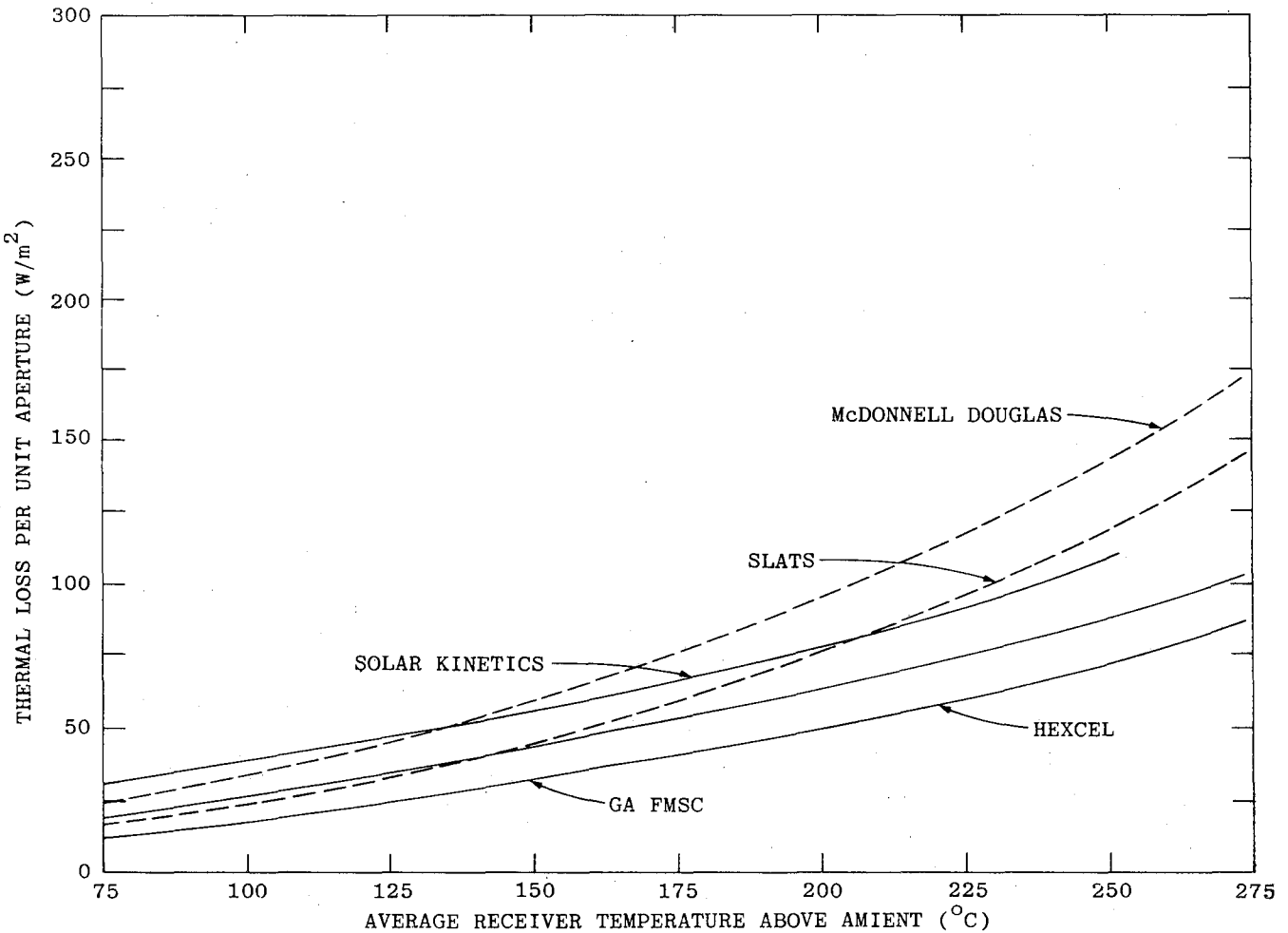

Figure 40. Comparison of Thermal Loss Per Unit Area Collector Aperture.

REFERENCES

1. Solar Total Energy Program Plan, SAND76-0167 (revised), August 1976, Sandia Laboratories, Albuquerque, New Mexico

2. Collector Module Test Facility, Fluid Loop Number 3, SAND78-0622 (to be published), Sandia Laboratories, Albuquerque, New Mexico

3. Zender, S. N., Sandia Solar Total Energy Test Facility Project, Final Report, Suntec 260 Square Meter SLATS Subsystem, SER 1022-60, December 1977, Sandia Laboratories, Albuquerque, New Mexico.

4. Performance Testing of the Suntec SLATS Solar Collector, SAND78-0623, (to be published), Sandia Laboratories, Albuquerque, New Mexico.

5. "Therminol 66, Technical Data Sheet, IC/FF-64," Monsanto Company.

6. Harrison, T. D., Dworzak, W. and Folkner, C., Solar Collector Module Test Facility, Instrumentation Fluid Loop Number One, SAND76-0425, January 1977, Sandia Laboratories, Albuquerque, New Mexico.

7. Parker, D., Test Results of Hexcel Parabolic Trough Solar Concentrator at Sandia Collector Module Test Facility, Document 178-DAP #1, January 1978, Hexcel Corporation, Dublin, California.

8. Dudley, V. E. and Workhoven, R. M., Performance Testing of the Hexcel Parabolic Trough Solar Collector, SAND78-0381, March 1978, Sandia Laboratories, Albuquerque, New Mexico.

9. Russell, J. L. Jr., DePlomb, E. P. and Bansal, R. K., Principles of the Fixed Mirror Solar Concentrator, GA-A12902, May 31, 1974, Gulf General Atomic, San Diego, California.

10. Eggers, G. H., Performance of the FMSC Test Modules, Final Report, Contract 05-6121, February 1978, Gulf General Atomic, San Diego, California.

11. Dudley, V. E. and Workhoven, R. M., Performance Testing of the General Atomic Fixed Mirror Solar Concentrator, SAND78-0624, April 1978, Sandia Laboratories, Albuquerque, New Mexico.

12. Dudley, V. E. and Workhoven, R. M., Performance Testing of the McDonnell Douglas Fresnel Lens Rotating Array Solar Collector, SAND78-0625, (to be published), Sandia Laboratories, Albuquerque, New Mexico.

13. Dudley, V. E. and Workhoven, R. M., Performance Testing of the Solar Kinetics Parabolic Trough Solar Collector, SAND78-0626, (to be published), Sandia Laboratories, Albuquerque, New Mexico.

DISTRIBUTION:
TID-4500-R66, UC62 (316)

Aerospace Corporation
P.O. Box 92957
Los Angeles, CA 90009
Attn: Richard Bruce

Aerospace Corporation
2350 E. El Segundo Blvd.
El Segundo, CA 90245
Attn: Leon Bush

Aerospace Corporation
101 Continental Blvd.
El Segundo, CA 90245
Attn: Elliott L. Katz

Acurex Aerotherm
485 Clyde Avenue
Mountain View, CA 94042
Attn: G. J. Neuner

American Gas Association
1515 Wilson Boulevard
Arlington, VA 22209
Attn: P. Susey

Solar Total Energy Program
American Technological University
P.O. Box 1416
Killeen, TX 76541
Attn: John J. Kincel, Director

Argonne National Laboratory (3)
9700 South Cass Avenue
Argonne, IL 60439
Attn: R. G. Matlock
W. W. Schertz
Roland Winston

Atlantic Richfield Co.
515 South Flower Street
Los Angeles, CA 90071
Attn: H. R. Blieden

Barber Nichols Engineering
6325 W. 55th Avenue
Arvada, CO 80002
Attn: R. G. Olander

Battelle Memorial Institute
Pacific Norhtwest Laboratory
P.O. Box 999
Richland, WA 99352
Attn: K. Drumheller

Brookhaven National Laboratory
Associated Universities, Inc.
Upton, LI, NY 11973
Attn: J. Blewett

Congressional Research Service
Library of Congress
Washington, DC 20540
Attn: H. Bullis

Del Manufacturing Co.
905 Monterey Pass Road
Monterey Park, CA 91754
Attn: M. M. Delgado

Desert Research Institute
Energy Systems Laboratory
1500 Buchanan Blvd.
Boulder City, NV 89005
Attn: Jerry O. Bradley

Desert Sunshine Exposure Inc.
P.O. Box 185
Phoenix, AZ 85020
Attn: Gene A. Zerlaut

Honorable Pete V. Domenici
Room 405
Russell Senate Office Bldg.
Washington, DC 20510

Edison Electric Institute
90 Park Avenue
New York, NY 10016
Attn: L. O. Elsaesser,
Director of Research

Energy Institute
1700 Las Lomas
Albuquerque, NM 87131
Attn: T. T. Shishman

EPRI
3412 Hillview Avenue
Palo Alto, CA 94303
Attn: J. E. Bigger

General Atomic
P.O. Box 81608
San Diego, CA 92138
Attn: J. L. Russell

General Electric Company
Valley Forge Space Center
Valley Forge, PA 19087
Attn: Walt Pijawka

General Electric Co.
P.O. Box 8661
Philadelphia, PA 19101
Attn: A. J. Poche

Georgia Institute of Technology
American Society of Mechanical
Engineers
Atlanta, GA 30332
Attn: S. Peter Kezios, President

Georgia Power Company
Atlanta, GA 30302
Attn: Mr. Walter Hensley
Vice President Economics Services

DISTRIBUTION (Cont)

Grumman Corporation
4175 Veterans Memorial Highway
Ronkonkoma, NY 11779
Attn: Ed Diamond

Hexcel
11711 Dublin Blvd.
Dublin, CA 94566
Attn: George P. Branch

Jet Propulsion Laboratory
Bldg. 277, Rm. 201
4800 Oak Grove Drive
Pasadena, CA 91103
Attn: V. C. Truscello

Lawrence Berkley Laboratory
University of California
Berkley, CA 94720
Attn: Mike Wallig

Lawrence Livermore Laboratory
University of California
P.O. Box 808
Livermore, CA 94500
Attn: W. C. Dickinson

Los Alamos Scientific Laboratory (2)
Los Alamos, NM 87545
Attn: J. D. Balcomb
MS 571 Q-DO
D. P. Grimmer
MS Q-11, Solar Group

Honorable Manuel Lujan
1324 Longworth Building
Washington, DC 20515

Mann-Russell Electronics, Inc.
1401 Thorne Road
Tacoma, WA 98421
Attn: G. F. Russell

Martin Marietta Aerospace
P.O. Box 179
Denver, CO 80201
Attn: R. C. Rozycki

McDonnell-Douglas Astronautics Co.
5301 Bolsa Avenue
Huntington Beach, CA 92647
Attn: Don Steinmeyer

NASA-Lewis Research Center
Cleveland, OH 44135
Attn: R. Hyland

New Mexico State University
Las Cruces, NM 88001
Attn: R. L. San Martin

Oak Ridge Associated Universities
P.O. Box 117
Oak Ridge, TN 37830
Attn: A. Roy

Oak Ridge National Laboratory
P.O. Box Y
Oak Ridge, TN 37830
Attn: J. R. Blevins
C. V. Chester
J. Johnson
S. I. Kaplan

Office of Science and Technology
Executive Office of the President
Washington, DC 20506
Attn: R. Balzhizer

Office of Technology Assessment
Old Immigration Building, Rm 722
119 D. Street, NE
Washington, DC 20002

Omnium G
1815 Orangethorpe Park
Anaheim, CA 92801
Attn: Ron Derby
S. P. Lazzara

Rocket Research Company
York Center
Redmond, WA 98052
Attn: R. J. Stryer

Honorable Harold Runnels
1535 Longworth Building
Washington, DC 20515

Honorable Harrison H. Schmitt
Room 1251
Dirksen Senate Office Bldg.
Washington, DC 20510

Scientific Atlanta, Inc.
3845 Pleasantdale Road
Atlanta, Georgia 30340
Attn: Andrew L. Blackshaw

Sensor Technology, Inc.
21012 Lassen Street
Chatsworth, CA 91311
Attn: Irwin Rubin

Solar Energy Research Institute
1536 Cole Blvd
Golden, CO 80401
Attn: C. J. Bishop
Ken Brown
B. L. Butler
Frank Kreith
Charles Grosskreutz

DISTRIBUTION (Cont)

Solar Energy Technology
Rocketdyne Division
6633 Canoga Avenue
Canoga Park, CA 91304
Attn: J. M. Friefeld

Solar Kinetics Inc.
P.O. Box 10764
Dallas, TX 75207
Attn: Gus Hutchison

Southwest Research Institute
P.O. Box 28510
San Antonio, TX 78284
Attn: Danny M. Deffenbaugh

Stanford Research Institute
Menlo Park, CA 94025
Attn: Arthur J. Slemmons

Stone & Webster
Box 5406
Denver, CO 80217
Attn: V. O. Staub

Sun Gas Company
Suite 800, 2 No. Pk. E
Dallas, TX 75231
Attn: R. C. Clark

Sundstrand Electric Power
4747 Harrison Avenue
Rockford, IL 61101
Attn: A. W. Adam

Suntec Systems Inc.
21405 Hamburg Avenue
Lakeville, MN 55044
Attn: J. H. Davison

Swedlow, Inc.
12122 Western Avenue
Garden Grove, CA 92645
Attn: E. Nixon

TEAM Inc,
8136 Ola Keene Mill Road
Springfield, VA 22152
Attn: Daniel Ahearne

Tennessee Energy Office
Suite 250, Capitol Hill Bldg.
Nashville, TN 37219
Attn: Carroll V. Kroeger, Sr.

U.S. Department of Energy
Agricultural & Industrial
Process Heat
Conservation & Solar Application
MS 2221C
20 Massachusetts Avenue NW
Washington, DC 20545
Attn: W. W. Auer

U.S. Department of Energy (3)
Albuquerque Operationis Office
P.O. Box 5400
Albuquerque, NM 87185
Attn: D. K. Nowlin
G. W. Rhodes
J. R. Roder

U.S. Department of Energy
Division of Energy Storage
Systems
4th Floor, RM 416
600 E. Street
Washington, DC 20545
Attn: C. J. Swet

U.S. Department of Energy (9)
Division of Solar Technology
Washington, DC 20545
Attn: R. H. Annan H. H. Marvin
G. W. Braun L. Melamed
M. U. Gutstein J. E. Rannels
G. M. Kaplan M. E. Resner
J. Weisiger

U.S. Department of Energy
Los Angeles Operations Office
350 S. Figueroa Street, Suite 285
Los Angeles, CA 90071
Attn: Fred A. Glaski

U.S. Department of Energy
San Francisco Operations Office
1333 Broadway, Wells Fargo Bldg.
Oakland, CA 94612
Attn: Jack Blasy

U.S. Department of Interior
Room 5204
Washington, DC 20204
Attn: M. Prochnik

University of Arkansas
Mechanical Engineering Dept.
Fayetteville, AR 72701
Attn: Dr. F. K. Deaver

University of Delaware
Institute of Energy Conversiuon
Newark, DE 19711
Attn: K. W. Boer

University of New Mexico (2)
Department of Mechanical Eng.
Albuquerque, NM 87113
Attn: W. A. Cross
M. W. Wilden

Watt Engineering Ltd.
RR1, Box 183 1/2
Cedaredge, CO 81413
Attn: A. D. Watt

DISTRIBUTION (Cont)

Western Control Systems
13640 Silver Lake Drive
Poway, CA 92064
Attn: L. P. Cappiello

Westinghouse Electric Corp.
P.O. Box 10864
Pittsburgh, PA 15236
Attn: M. K. Wright
J. Buggy

1100 C. D. Broyles
1260 K. J. Touryan
1262 H. C. Hardee
1280 T. B. Lane
1284 R. T. Othmer
1300 D. B. Shuster
1330 R. C. Maydew
2300 J. C. King
2320 K. L. Gillespie
2323 C. M. Gabriel
2324 L. W. Schulz
2326 G. M. Heck
3161 J. E. Mitchell
3700 L. S. Conterno
5000 A. Narath
5200 E. H. Beckner
5231 J. H. Renken
5700 J. H. Scott
5710 G. E. Brandvold
5711 J. F. Banas
5712 J. A. Leonard
5713 B. W. Marshall
5714 R. P. Stromberg
5715 R. H. Braasch
5719 D. G. Schueler
5730 H. M. Stoller
5740 V. L. Dugan
5800 R. S. Claassen
Attn: R. G. Kepler, 5810
R. L. Schwoebel, 5820
5830 M. J. Davis
5831 N. J. Magnani
5834 D. M. Mattox
5840 H. J. Saxton
5842 J. N. Sweet
5844 F. P. Gerstle
5846 E. K. Beauchamp
8100 L. Gutierrez
8130 R. C. Wayne
8131 W. G. Wilson
8132 A. C. Skinrood
8266 E. A. Aas
8313 R. W. Mar
9330 A. J. Clark, Jr.
9340 W. E. Caldes
9350 F. W. Neilson
9352 O. N. Burchett
9400 H. E. Lenander
9572 L. G. Rainhart
9700 R. E. Hopper
Attn: H. H. Pastorius, 9740
R. W. Hunnicutt, 9750

3141 C. A. Pepmueller (5)
3151 W. L. Garner (3)
For DOE/TIC
(Unlimited Release)
6011 G. C. Newlin